

New Classical and Bayesian Estimators for Classifying Trade Direction in the absence of Quotes

Michael Bowe^{a,b}, Sungjun Cho^a, Stuart Hyde^a and Iljin Sung^a

This Draft: May 2018

We propose new methods for estimating the effective bid-ask spread and classifying trading intentions without access to quotes. Our state space approach utilizes both classical and Bayesian estimators. We extend Hasbrouck's (2004) methodology by simultaneously allowing for both unbalanced and autocorrelated order flow, and a role for informational asymmetry. Our methods are easy to implement in practice and provide simple parametric alternatives to both the nonparametric bid-ask spread estimators proposed by Chen, Linton, Schneeberger, and Yi (2016) and the various trade classification algorithms discussed in Easley, Lopez de Prado and O'Hara (2016). For illustrative purposes, we apply our approach to an analysis of the trading patterns in the CME's gold futures contract during a period incorporating uncertainty in financial markets as a result of the UK's 2016 Brexit referendum.

^a Division of Accounting and Finance, Alliance Manchester Business School, University of Manchester, Booth Street East, Manchester, M13 9SS, UK. email: mike.bowe@mbs.ac.uk, sungjun.cho@mbs.ac.uk, stuart.hyde@mbs.ac.uk, iljin.sung@manchester.ac.uk

^b Department of Accounting and Finance, University of Vaasa, Wolffintie 34, 65200 Vaasa, Finland.

We wish to acknowledge the comments of Ian Garrett, Julian Williams and Sarah Zhang on earlier drafts of this paper.

1. INTRODUCTION

A variety of approaches exist in the literature to compute accurate estimates of trading costs in financial markets in order to evaluate the impact of changing liquidity conditions on market performance. These liquidity proxies are typically computed based on quotes and employ various methods of assigning trading intentions, where a trade is classified as a buy (sell) if the active (i.e., liquidity consuming) side of the trade is a buyer (seller). Trade direction indicators based on such classifications are then used to measure the information content of trades (e.g., Hasbrouck (1991)) and to predict liquidity crashes (e.g., Easley, Lopez de Prado and O'Hara (2012)).

Accurately estimating liquidity often proves to be an elusive task. A major obstacle relates to the stipulations placed on the data, since liquidity estimates often require accurate observations on both intra-daily bid-ask quotes and transaction prices. As a result, trade classification is never straightforward. Historically, the Lee and Ready (1991) algorithm (LR), based on both quote and price changes, is the most popular trade classification algorithm. However, recent literature suggests that with the advent of high frequency trading in markets, the accuracy of LR algorithm is potentially undermined. For example, Easley, Lopez de Prado and O'Hara (2016) argue that in electronic limit order markets, some with order cancellation rates of 98% or more, trade classification algorithms based on proximity to bid and ask quotes are severely compromised. Holden and Jacobsen (2014) using the TAQ data, and Panayides, Shohfi, and Smith (2014) employing Euronext Paris data provide empirical support for these claims. Furthermore, as Holden, Jacobsen, and Subrahmanyam (2015) observe, the trading environment in many financial markets (such as futures and foreign exchange trading) lacks transparency, in the sense actual quotes are not directly observable in the intra-daily data record. Such information must somehow be discerned from the data.

To overcome these data limitations requires developing an empirical methodology to extract a liquidity proxy and classify trading intentions without access to quotes. In this regard, Hasbrouck (2004) develops both a liquidity measure and trade classification algorithms in the absence of quotes using variations of the Roll (1984) model, proposing a new Bayesian approach by assuming an i.i.d. normal distribution for price innovations and latent independent trade indicators. Four representative CME futures contracts illustrate application

of the methodology. Subsequently, Van der Wel, Menkeld, and Sarkar (2009) develop the equivalent classical maximum likelihood estimation (MLE) methods by mapping the Roll model onto the regime switching state space model of Kim and Nelson (1999).

Chen, Linton, Schneeberger, and Yi (2016) document several concerns with the Hasbrouck (2004) approach, including its assumptions of normal price innovations, balanced market order flow, the absence of serial correlation in the trade direction indicators, symmetric information, and constant spreads within the sample period (e.g., for a month). They argue these assumptions could lead to inaccurate estimates, at least during certain trading episodes. These reservations lead Chen, Linton, Schneeberger, and Yi (2016) to propose new nonparametric methods for estimating the bid-ask spread using only transaction prices. Initially, they relax the normality assumption for prices innovations using an empirical characteristics function while maintaining the other assumptions of the Hasbrouck (2004) method. They find that their method produces nearly identical results to the Roll (1984) and Hasbrouck (2004) methods during normal times but performs much better during periods of extreme turbulence. Specifically, analyzing movements in the E-mini futures contract on the S&P 500 during the Flash Crash, they discover that while their estimator is comparable to other methods during most of Flash Crash day, during its peak period, i.e., between 2:45 pm and 2:49 pm ET, their spread estimates seem to provide better approximations. The paper also suggests how their proposed framework can accommodate certain other extensions, such as: unbalanced order flow, serially dependent latent trade indicators, or adverse selection. However, there are several caveats to their approach. First, no empirical analysis is undertaken involving these extensions, possibly reflecting the pervasive curse of dimensionality when applying such nonparametric methods. Second, they develop each extension in isolation, without simultaneously relaxing the limiting features they identify in prior models. Finally, as their focus is on developing new methods to estimate the bid-ask spread, they do not provide a filtering algorithm to obtain the latent trade direction indicators.

The central contribution of this paper is to develop easy-to-implement Bayesian and MLE estimators by extending both Hasbrouck (2004) and Van der Wel, Menkeld, and Sarkar (2009) to simultaneously accommodate several of the omitted features evaluated in Chen, Linton, Schneeberger, and Yi (2016), namely unbalanced and autocorrelated order flow and informational asymmetries.

The second major contribution of this paper is to provide trade direction classification mechanism without recourse to quotes. These classification systems utilise both Bayesian MCMC methods and classical filtering and smoothing algorithms for latent trade direction indicators. Recently, Easley, Lopez de Prado, O'Hara (2016) propose a new conceptual framework for classifying trades, taking the perspective of a Bayesian statistician with priors on the unobservable information (buy or sell indicator), who is trying to extract trading intentions from observable trade data. They compare the strengths and weakness of several rules against an ideal Bayesian rule. We propose that certain familiar structural empirical market microstructure models, such as those we employ in this analysis, provide plausible approximations to their ideal Bayesian trade classification approach. In particular, these models employ a Markov switching process as the underlying process governing the dynamics of the unobservable buy-sell indicator, and treat the measurement equations as a plausible data generating process for the observed data relating to the indicator. Thus, we propose using estimates of the autocorrelated trade direction indicators, or the buy-sell indicator, as the model consistent, trade classification algorithm.

For purposes of illustration, we apply our proposed approach to analyse trading behaviour in the gold futures contract trading on the CME over the two month period from May 2016 to June 2016, a timeframe incorporating the UK Brexit referendum. Specifically, we first estimate the effective spread, and subsequently decompose it into non-informational and informational components, computing daily correlation estimates of classified trades between our model-consistent trade classification rules and those we obtain from the Tick rule.

The main findings are as follows. First, we obtain almost identical results from both classical MLE and Bayesian methods in all empirical models throughout the sample period. Second, we find estimates of daily trade direction indicators to be highly autocorrelated, leading to measured bid-ask spreads being larger, in an economically meaningful sense, than those obtained from alternative estimates employing independent trade direction indicators. Third, we find strong statistical support for asymmetric information models of the type proposed by Glosten and Harris (1988) in the presence of latent and autocorrelated trade direction indicators. The results provide evidence that the trade impact coefficients implied by the asymmetric information model, which reflect Kyle's lambda, are important elements of liquidity. Fourth, when comparing the Roll model and Tick rule we find that the daily

correlation estimates of the classified trades are almost always above 0.99, indicating that the trade classification we obtain from the Roll model used in Hasbrouck (2004) and the Tick rule are essentially identical. Finally, our model consistent trade classification algorithm based on an extended GH model provides very similar results to the Tick rule during normal trading periods. However, in the presence of greater uncertainty when trading potentially generates a greater price impact (relating from to order flow imbalances), our trade classification indicator often diverges significantly from those we obtain using the Tick rule.

As Easley, Lopez de Prado, and O'Hara (2016) maintain that Tick rule classifications appear particularly problematic in periods of high volatility exhibiting imbalances in order flow, we believe the approach to trade classification we propose shows some promise. Importantly, we do not claim that our trade classification system is superior to other rules. As Easley, Lopez de Prado, and O'Hara (2016) note, each trade classification rule may demonstrate both strengths and weakness, depending on the underlying market characteristics. Instead, we maintain that our approach may be best suited to classifying trades consistently in environments where a variant of state space models with regime switching yields a realistic approximation to the trading conditions. Moreover, our methods have the advantage of providing easy-to-implement model consistent trade classification algorithms using both Bayesian and Classical estimation methods. As such, we believe they may be a useful addition to the empirical microstructure tool kit.

The remainder of this paper is organized as follows. Section 2 briefly reviews the Roll (1984) structural market microstructure model and its subsequent generalizations leading to richer information-based models. Our focus here is on resolving estimation issues linked to the model parameters. Section 3 presents the classical and Bayesian estimation methods we propose. We outline data sources and present and discuss the main empirical results in section 4. Section 5 concludes the paper.

2. Empirical Structural Market Microstructure Models

2.1. The Roll model

The Roll (1984) model is a parsimonious structural market microstructure model of the bid-ask spread. The model decomposes the dynamics of the asset pricing process into two components, namely: (i) changes in the “efficient price” reflecting the fundamental value of the security conditional on all publicly available information, and (ii) the costs associated with the trading process. This model is initially derived by assuming a competitive dealer market with fixed transaction costs and symmetric information, in which dealers set their bid-ask quotes to recover their costs of making a market. However, in modern financial markets, high frequency trading firms typically act as market makers, by placing passive orders at various levels of the order book to earn tiny margins on large bets (Easley, Lopez de Prado, O’Hara (2012)). Indeed, Hendershott and Menkveld (2014) propose a more general definition of liquidity suppliers (market makers) in modern financial markets as agents who trade against price pressures. This interpretation of the market maker is consistent with the Roll model, where the market maker buys at a discount (negative price pressure) and sells at a premium (positive price pressure).

The price dynamics in the Roll model can be represented as follows. Denote the efficient price by M_t with $\log(M_t) = m_t$ and the transaction price by P_t with $\log(P_t) = p$. The evolution of these two prices can be depicted as:

$$p_t = m_t + cq_t, \quad m_t = m_{t-1} + u_t, \quad u_t \sim N(0, \sigma_u^2) \quad (1)$$

where q_t is a regime switching variable with $q_t \in \{-1, +1\}$ and

$$\Pr[q_t = 1 | q_{t-1} = 1] = 0.5, \Pr[q_t = -1 | q_{t-1} = -1] = 0.5.$$

The Roll model contains two sources of randomness. It assumes the efficient price evolves as a random walk, with the i.i.d. innovation term (u_t) reflecting public information. The trade direction indicator q_t is a random variable taking one of two values, +1 (-1) for a buyer (seller) initiated trade. Buyer and seller initiated trades are assumed to be equally probable, and in the Roll model q_t is independent of u_t , so the direction of trade is independent of

changes in the efficient price. This effectively eliminates any influence of asymmetric information in the model, and it is one of the key assumptions we relax later in the paper. The term c is interpreted as the (log of) the effective execution cost paid by an active buyer or seller. The Roll specification implies:

$$\Delta p_t = m_t + cq_t - m_{t-1} - cq_{t-1} = c\Delta q_t + u_t, \quad (2)$$

Roll proposes a moment estimator to compute estimates of bid-ask spreads based only on transaction prices. However, Roll's estimate is feasible only if the first-order sample autocovariance is negative and as a result Roll's reported spread estimator is often biased downward. To reduce this downward bias, Hasbrouck (2004) proposes a Bayesian method to estimate model parameters, assuming normal distributions characterise the innovation term (u_t) and latent independent trade indicators. Van der Wel, Menkveld, and Sarkar (2009) develop alternative classical MLE methods for the Hasbrouck (2004) model, and Chen, Linton, Schneeberger, and Yi (2016) use nonparametric methods to relax the normality assumption. . However, Chen, Linton, Schneeberger, and Yi (2016) also point out several remaining problems with these econometric approaches, such as the assumptions of balanced market order flow, symmetric information and the absence of serial correlation in the trade direction indicators. In the following section we proceed to relax these assumptions and provide an extension to the econometric methods developed by Hasbrouck (2004) and Van der Wel, Menkveld, and Sarkar (2009).

2.2 Generalizations of the Roll model

(i) Autocorrelation in order arrival and unbalanced market order flow

Choi, Salandro and Shastri (1988) provide several reasons, such as information disclosure concerns leading to strategic trading behaviour (order fragmentation), for the existence of serially correlated trade arrival in financial markets, and extend the Roll model to incorporate autocorrelated trade direction indicators. In this paper we use the following model (henceforth the extended Roll model (MS)) to accommodate these stylised facts.

$$p_t = m_t + cq_t, m_t = m_{t-1} + u_t, u_t \sim N(0, \sigma_u^2) \quad (3)$$

where the trade direction indicator, q_t is a random variable taking values of 1 or -1, governed by the following Markov process:

$$\Pr[q_t = 1 | q_{t-1} = 1] = P \quad \text{and} \quad \Pr[q_t = -1 | q_{t-1} = -1] = Q$$

(ii) Adverse selection

Easley, Lopez de Prado, and O'Hara (2012, p.1457) define adverse selection in modern limit order markets as the “natural tendency for passive orders to fill quickly when they should fill slowly and fill slowly (or not at all) when they should fill quickly”. They also explain that such a definition is consistent with market microstructure models proposed by Glosten and Milgrom (1985) and Kyle (1985). In these models, order flow is informative for subsequent price moves as it reflects the level of informed trading. These models provide insights into the behaviour of market participants in the presence of informational asymmetries and motivate further modifications to the original Roll model. These modifications allow the efficient price to be at least partially driven by the trade direction indicator variable, capturing a key feature of asymmetric information microstructure models, namely that trade characteristics may convey information correlated with a trader's private information.

To accommodate the above stylised features of trading, we propose a model extension which incorporates both a term capturing latent and autocorrelated trade direction indicators and an additional one reflecting potential adverse selection costs.. In this model, only the unexpected component of the trade direction indicator series produces any effect on the efficient price. We represent this model (henceforth the extended GH model (GH)) as follows:

$$p_t = m_t + cq_t, m_t = m_{t-1} + (\lambda_0 + \lambda_1 \sqrt{V_t}) (q_t - E[q_t | \psi_{t-1}]) + u_t, u_t \sim N(0, \sigma_u^2) \quad (4)$$

where λ_0 and λ_1 represent that fixed and variable permanent price impact costs, respectively, and ψ_{t-1} denotes the available information set, up to time $t-1$. The trade direction indicator, q_t , follows the Markov process in (3). Following a straightforward reformulation, we can express this process as the autoregressive (AR) process.

$$q_{t+1} = (P - Q) + (P + Q - 1) q_t + \varepsilon_{t+1}, E[\varepsilon_{t+1} | q_t] = 0 \quad (5)$$

This formulation of the AR(1) process for the trade direction indicators is used previously in the literature on several occasions (e.g., Madhavan, Richardson, and Roomans (1997)). In summary, in our proposed model, $E[q_t | \psi_{t-1}]$ can be expressed as $(P-Q)+(P+Q-1)q_t$, and in its final form, the empirical model we estimate may be depicted as follows:

$$\begin{aligned} p_t &= m_t + cq_t, \\ m_t &= m_{t-1} + (\lambda_0 + \lambda_1 \sqrt{V_t})(q_t - \mu - \rho q_{t-1}) + u_t, \quad u_t \sim N(0, \sigma_u^2) \end{aligned} \quad (6)$$

where $q_t = \{1, -1\}$, $\Pr[q_t = 1 | q_{t-1} = 1] = P$, $\Pr[q_t = -1 | q_{t-1} = -1] = Q$ and $\mu = P - Q$, $\rho = P + Q - 1$.

The model has a reduced form representation, given by:

$$\Delta p_t = c \Delta q_t + (\lambda_0 + \lambda_1 \sqrt{V_t})(q_t - \mu - \rho q_{t-1}) + u_t, \quad u_t \sim N(0, \sigma_u^2) \quad (6')$$

In this framework, the market-maker requires compensation not only for the costs of processing an order (c) as in the Roll model, but also for the adverse selection risk of supplying liquidity to an informed trader, where $\lambda_1 \sqrt{V_t}$ captures the adverse selection component of a trade's price impact. The literature has a variety of interpretations of the coefficient λ_1 from a measure of Kyle's lambda, the slope of the price impact curve arising from asymmetric information effects, to the (inverse) market depth parameter (Brennan and Subrahmanyam (1996)). Prior to proceeding, we note that Chen, Linton, Schneeberger, and Yi (2016) provide several theoretical extensions of their model, selectively incorporating unbalanced order flow, serially dependent latent trade indicators, and adverse selection. However, in contrast to the present model formulation, no attempt is made to simultaneously accommodate these features, and they do not conduct any extensive empirical analyses.

3. Estimation Methods for Structural Market Microstructure Models

Van der Wel, Menkveld, and Sarkar (2009) show that the Roll model used in Hasbrouck (2004) can be interpreted as a state space model. For example, one natural interpretation of equation (3) is a state space system with measurement and transition equations as follows:

Measurement equation: $p_t = m_t + cq_t, q_t \in \{-1, +1\}$

Transition equation: $m_t = m_{t-1} + u_t, u_t \sim N(0, \sigma_u^2)$

Employing the same reasoning, we can reformulate the extended GH model with asymmetric information (equation (6)) as a state space model, with associated equations given by:

Measurement equation: $p_t = m_t + cq_t$

Transition equation: $m_t = m_{t-1} + (\lambda_0 + \lambda_1 \sqrt{V_t}) (q_t - ((P-Q)+(P+Q-1)q_{t-1})) + u_t$

Recently, many papers adopt similar state space formulations to estimate market microstructure models. For example, Menkveld, Koopman, and Lucas (2007) model a high-frequency price series as the sum of efficient price series, reflecting permanent price effects as above, and stationary series capturing transitory price effects. A similar framework also is subsequently adopted in Menkveld (2013), Brogaard, Hendershott, and Riordan (2014), and Hendershott and Menkveld (2014).

3.1. Bayesian Markov chain Monte Carlo (MCMC) methods

Hasbrouck (2004) develops a Bayesian Gibbs sampling approach to estimating the Roll model with normality assumption governing price innovations (equation (3)), in which the parameters (c and σ_u) are considered to be random variables (reflecting the statistician's uncertainty). He motivates the technique's adoption with reference to its ability to accommodate important economically meaningful latent data such as trade direction indicators ($q = \{q_1, q_2, \dots, q_T\}$), which are "suppressed in the GMM estimation" (Hasbrouck 2004, p.311). Inference is based upon a series of transaction prices through time: $p = \{p_1, p_2, \dots, p_T\}$, with knowledge of $q = \{q_1, q_2, \dots, q_T\}$ and p sufficient to determine the efficient price, $m = \{m_1, m_2, \dots, m_T\}$. The respective joint distribution function $F(c, \sigma_u, q | p)$, summarizes the full posterior over parameters and latent data. To estimate the present model, we use Hasbrouck's MatLab codes available in his website (<http://people.stern.nyu.edu/jhasbrou/>).

In this paper, we extend the Roll model of Hasbrouck (2004) by adding unbalanced order flow and autocorrelated trade direction indicators. Our extension (equation (4)) has two extra

transition probability parameters (P and Q) and $F(c, \sigma_u, q, P, Q | p)$ summarizes the full posterior over parameters and latent data. While there is no tractable closed-form representation for this joint distribution function, $F(c, \sigma_u, q, P, Q | p)$, the full conditional (posterior) distributions for the parameters are often tractable. In estimating both equations (3) and (4), for example, conditional on q , the equation $\Delta p_t = c \Delta q_t + u_t$ can be treated as a simple normal linear regression specification in which c and σ_u are the regression coefficient and residual standard deviation, respectively. It is also possible to express the conditional distribution of q based on the model parameters and data. The major differences between Hasbrouck's (2004) Gibbs sampling algorithm and the Gibbs sampling method we adopt to estimate the model in equation (4) arises in relation to the simulation of q_t .¹

The power of Bayesian analysis using the Gibbs sampler is that it requires only the conditional distributions to numerically recover the joint distribution function. The Gibbs sampler is an iterative procedure of drawing each parameter, or latent trade direction indicator, sequentially. Initially, the parameters and latent trade direction indicators are set equal to some arbitrary values $\{c^{(0)}, \sigma_u^{(0)}, q^{(0)}, P^{(0)}, Q^{(0)}\}$, although efficient estimation typically requires specifying reasonable starting values, such as GMM estimates of $(c$ and $\sigma_u)$, whenever they are available. In the subsequent iterations, all parameters and latent trade direction indicators except for the component being drawn are taken as given, and each component is updated sequentially. For example, the second iteration starts with a draw of $c^{(2)}$ conditional on $(\sigma_u^{(1)}, q^{(1)}, P^{(1)}, Q^{(1)})$. By repeating this procedure we generate a sequence of draws of unknowns for $j=1, \dots, n$. The Gibbs principle demonstrates that the limiting distribution of the n^{th} draw after burn-in samples (as $n \rightarrow \infty$) is $F(c, \sigma_u, q, P, Q | p)$, the desired posterior, and the limiting draw for any parameter is distributed as the corresponding marginal posterior. For example, the limiting density of $c^{(n)}$ is $f(c | p)$. The number of simulation must be sufficiently large so that dependence on the initial conditions becomes insignificantly small.

¹ We explain the details of the Gibbs sampling algorithms for these two methods and the differences between them in Appendices A1 and A2.

In any MCMC estimation, it is crucial to ensure convergence of the chain in order to undertake correct statistical inference. In this paper, as a diagnostic to check for the convergence of our MCMC algorithm, we compute and report the effective sample size based on the inefficiency factors and the p-value of Geweke's (1992) convergence diagnostics test for the model parameters.² Finally, based on the simulation outputs, we estimate population parameters of the posterior using standard time series analysis techniques, noting that the sample mean of $c^{(j)}$ is a consistent estimate of $E[c|p]$ and the sample variance is a consistent estimate of $Var[c|p]$. We can also interpret trade direction indicators we estimate as outputs from a model-consistent trade classification algorithm.

To estimate the most complex model which incorporates adverse selection (equation (6)), we need to develop a new Bayesian Algorithm to simulate iteratively $F(c, \lambda_0, \lambda_1, \sigma_u, P, Q, q|p)$. This is for the following reasons. First, the innovation in autocorrelated q_t impacts the efficient price. Second, this model involves two extra parameters capturing the price impact of trades (λ_0, λ_1), while the two transition probabilities (P and Q) also appear in the regression specification. The implication is that we cannot use the customary Gibbs sampling estimation algorithm to estimate these parameters. In response, we develop a tailored random walk Metropolis Hastings algorithm to undertake this task.³

3.2 Classical MLE methods

Van der Wel, Menkveld, and Sarkar (2009) develop alternative MLE methods for Hasbrouck's (2004) Roll model formulation (equation (3)). In this paper, we extend their approach in two ways. First we incorporate order flow imbalances and autocorrelated trade direction indicators (equation (4)), and second, we include an adverse selection term (equation (6)). We can interpret these models as state space models with regime switching, as explained in the previous section. In ordinary state space models with normally distributed

² We provide more details in Appendix B.

³ We present the details in Appendix A3.

shocks, a Kalman filtering technique is employed to construct the likelihood function utilising prediction error decomposition. However, several models used in this paper incorporate a discrete regime switching variable (q_t). In such cases, Kim and Nelson (1999) demonstrate we can estimate the model with a composite filter, which is a combination of a Kalman and a Hamilton filter. Based on this nonlinear filter we obtain an approximate likelihood function, and utilise MLE methods for estimation.⁴ One critical issue with this approach is that it is difficult to precisely quantify the bias caused by using this approximate filter. Fortunately, we can avoid undertaking the approximation by expressing several models in their reduced form. For example, as previously shown (equation (6')), the extended GH model with asymmetric information can be written as:

$$\Delta p_t = c\Delta q_t + (\lambda_0 + \lambda_1 \sqrt{V_t}) (q_t - ((P-Q) + (P+Q-1)q_{t-1})) + u_t$$

On this basis, we can interpret this version of the extended GH model as a standard regime switching model and use a Hamilton filter to construct likelihood function values.⁵

3.3 Discussion of the estimated trade direction indicator, q_t

Our core proposal is that the autocorrelated trade direction indicators, q_t , we estimate from the previous models can be considered to be model consistent trade classification algorithms. Specifically, we can directly recover the trade direction indicator, q_t , from the outputs of Bayesian estimation, while for classical MLE methods, we can employ filtering and smoothing algorithms to compute the probability of q_t for each trade. In other words, once we estimate the empirical market microstructure models we present in this paper, we can determine whether each trade is initiated by a buyer ($q_t = 1$) or a seller ($q_t = -1$).

We note earlier that the advent of high frequency trading platforms calls into question the accuracy of traditional trade classification systems such as the Lee and Ready (1991) algorithm (LR In lieu, Easley, Lopez de Prado, O'Hara (2016) propose a new conceptual

⁴ Chapter 5 of Kim and Nelson (1999) provides more details.

⁵ We provide precise details of how we implement MLE methods for estimation in Appendix C.

framework for classifying trades. They adopt the perspective of Bayesian statisticians with priors on the unobservable information (here q_t), who are trying to extract trading intentions from observable trading data. Ideally, we would like to specify the data generating processes for both the underlying unobservable variables and subsequently for the observed data, conditional on the realizations of the underlying unobservable data. Formulating such specifications may prove a daunting task, and computing closed-form solutions for conditional probabilities is likely to be complex, even when such solutions exist. They claim that every trade classification algorithm can be regarded as an approximation to this Bayesian approach, and that their bulk volume classification (BVC) methodology is conceptually closer to this ideal than traditional approaches such as the Tick rule, since BVC assigns a probability to a given trade being either a buy or sell.

We believe that the empirical market microstructure models we outline in this paper provide another plausible approximation to the ideal Bayesian trade classification approach. For example, in relation to equations (3) and (6), we can interpret the relevant transition equations as the data generating process for the underlying unobservable variables, q_t , and the measurement equations as the plausible data generating process for the observed data relating to q_t . While the extent to which these empirical market microstructure models capture market reality remains unclear, much research employs these models as the empirical basis for their investigations in this area.⁶

Note, we do not claim that our trade classification system is generally superior to other existing rules such as the Tick and BVC rules. As Easley, Lopez de Prado and O'Hara (2016) maintain, each trade classification rule may have advantages which are only manifest in differing trading environments: with less noisy data the Tick rule may prove to be generally superior to the BVC, while with noisy data the BVC may prevail. We believe that our approach is better suited to situations where a variant of state space models incorporating regime switches better approximates the dynamics of the trading environment. In such situations, our proposed methods provide model consistent trade classification algorithms using both Bayesian and Classical methods which are easy to implement in practice.

⁶ Hasbrouck (2007) provides a comparative summary of relevant literature.

4. EMPIRICAL ANALYSIS

4.1 Data description

We conduct the empirical implementation of our proposed trade classification methods using data from gold futures trading on the Chicago Mercantile Exchange (CME) during May and June 2016. We select this particular asset and time period for the following reasons. First, gold futures (ticker symbol GC), are among the most widely traded of all futures contracts worldwide, and gold is often considered a “safe haven” asset at times of global economic uncertainty, such as the period surrounding the UK’s Brexit referendum on June 23, 2016 which we deliberately include in our sample for precisely this reason. Second, as Easley, Lopez de Prado, and O’Hara (2016) explain, the gold futures market is less fragmented than its spot market. Each contract trades on a single market, and trading data is less noisy, since all trades are mandated to occur at either the best bid or the best offer and trades between the spread are not permitted. Further, while New York futures volume is less than a tenth of the London spot volume, the futures contract plays the key role in the process of price discovery, leading the spot market in incorporating new, gold price-relevant information into asset values, (Hauptfleisch, Putnin, and Lucey (2016)).

Specifically, we select our sample data from the gold futures contract trading on CME’s Globex electronic trading platform during the period from May 1, 2016 to June 30, 2016. Electronic trading on CME Globex is available virtually 24 hours a day from Sunday 6:00 p.m. through to Friday 5:00 p.m. Eastern Standard Time (EST)⁷, with only a 60-minute break each day beginning at 5:00 p.m. EST⁸. For the empirical analysis, with reference to trading volume, we identify the most actively traded gold futures contract on any given day to construct a continuous series. The most active gold futures contract from May 1 to May 26 is the June contract deliverable on any business day in June 2016 (GCM6). On May 27 volume shifts to another contract deliverable during August 2016 (GCQ6). The transaction price series and trading volume data, time-stamped to the microsecond, are sourced from the

⁷ Thus, the trading activity on any given date starts at 6:00 p.m. and finishes at 5:00 p.m. EST the following day. For example, on May 1 trading starts at 6:00 p.m. on May 1 and finishes at 5:00 p.m. on May 2.

⁸ There is one exception during our sample period: trading on Globex halted at 1:00 p.m. and reopened at 6:00 p.m. on Monday, May 30, 2016 because of the Memorial Day holiday trading schedule.

Thomson Reuter Tick History (TRTH) database. When several orders are time-stamped to the same microsecond they are aggregated to obtain volume-weighted prices and total volumes. Finally, following Marshall, Nguyen, and Visaltanachoti (2012), we winsorize all return variables at the 0.5% and 99.5% levels so data errors are not driving the results.⁹

Table 1 describes relevant features of the gold futures contracts. Each gold futures contract represents 100 troy ounces and is quoted in US dollars per troy ounce. Minimum tick size on the contract is 10 cents per troy ounce. As a proportion of the contract price, average tick size is 0.008% and the standard deviation of the price change is approximately 7 ticks after winsorization at the 0.5% and 99.5% levels. The contracts evidence a fast pace of trading activity, with an average 1.6 seconds between trades. Figure 1 illustrates the daily series of average prices and trading volumes during the sample period.

4.2 The Roll model

As our benchmark, we estimate the Roll model each day during our sample period, using both Hasbrouck's (2004) Bayesian, and Van der Wel, Menkveld and Sarkar's (2009) MLE models. To clarify notation and facilitate ensuing discussions, we re-state the Roll model as:

$$p_t = m_t + cq_t, \quad m_t = m_{t-1} + u_t, \quad u_t \sim N(0, \sigma_u^2)$$

where q_t is a regime switching variable with $q_t \in \{-1, +1\}$ and

$$\Pr[q_t = 1 | q_{t-1} = 1] = 0.5, \Pr[q_t = -1 | q_{t-1} = -1] = 0.5.$$

All model parameters are assumed to be constant during any given day, but can change across days. To guarantee accurate statistical inference, we implement the Bayesian estimations with a 100,000 iteration burn-in period and 250,000 total iterations, increasing these numbers by 10,000 until we simultaneously satisfy both the convergence criteria for the inefficiency factors and Geweke's (1992)'s diagnostic tests for all parameters¹⁰.

⁹ Marshall, Nguyen, and Visaltanachoti (2012) clean the data in two steps. They first compute the 5% -trimmed sample mean and standard deviation for each high-frequency liquidity measure, meaning the top and bottom 5% observations are excluded from the trimmed mean and standard deviation calculations. Then they remove observations that are outside the trimmed mean by +/- three standard deviations.

¹⁰ Refer to Appendix B for more details on the inefficiency factors and the Geweke (1992) diagnostic tests. Table A.1 (the column 'Roll (Bayesian)') indicates that convergence criteria are achieved for the Roll model, since the effective size exceeds 1,000 and Geweke's (1992) p-values are greater than 0.05 for all parameters.

[Table 2 in here]

Table 2 reveals that we obtain benchmark MLE estimates very close to the Bayesian estimates, validating the use of MLE methods in estimating the model. Computing the daily differentials between the estimates of c and σ_u we obtain from the two methods, the average value is zeros and the maximum of the absolute differential values is minuscule (0.1×10^{-7})¹¹, confirming the methods provide almost identical estimates. The averages of the percentage effective half spread, c , and the standard deviations, σ_u , are 0.26×10^{-4} and 0.43×10^{-4} , respectively. Noteworthy is the fact that on the day of the UK's Brexit referendum (June 23), the estimate of c is 0.33×10^{-4} , one of the largest values in the sample, while that for the standard deviation, σ_u , is 0.96×10^{-4} , an increase of close to 90% when compared to its value the previous day.

4.3 The Roll model with autocorrelated q_t : a simulation exercise

We now proceed to introduce autocorrelated trade direction indicators into the analysis, by re-stating the extended Roll model as:

$$p_t = m_t + cq_t, \quad m_t = m_{t-1} + u_t, \quad u_t \sim N(0, \sigma_u^2)$$

where q_t is a regime switching variable with $q_t \in \{-1, +1\}$, and to capture autocorrelation in the trade direction indicators we specify:

$$\Pr[q_t = 1 | q_{t-1} = 1] = P, \Pr[q_t = -1 | q_{t-1} = -1] = Q$$

Simulations are undertaken both to validate the computational accuracy of our estimations and to compare the results we obtain using alternative approaches to estimation. To establish a sound basis for a plausible data generating process in the simulations, we generate the data employing the averages of the parameter estimates we report in Table 4, on the assumption that the trade direction indicator is autocorrelated and has persistent regimes. To minimize simulation errors, for each model we generate the data 50 times, and estimate the parameters and trade direction indicators for each data sample, enabling us to compute simulated sample averages. We then compare the estimation results from the MLE approach with those from our proposed Bayesian Gibbs sampling methods.

¹¹ Table A.2 provides further details..

[Table 3 in here]

Table 3 presents the results from these simulations. The estimates of the standard deviation of changes in the (log) efficient price and the (log) half-spread are σ_u and c , respectively. Finally, P and Q are the transition probabilities of the latent regime switching process for the trade direction indicators. The results we label “Bayesian” derive from the Bayesian Gibbs sampler in which trade direction indicators are conditionally simulated and autocorrelated. The results are based on 12,000 sweeps of the sampler, with the first 2,000 discarded. We obtain the alternative estimates MLE estimates applying classical MLE methods to the regime switching models. Once again, we conclude that both methods provide estimates close to the true parameter values we use in the simulations.

4.4 The Roll model with autocorrelated q_t : gold futures contract estimation

We believe the outcome of the simulation exercises in section 4.3 enable us to confirm the integrity of our chosen estimation methodology, so, using the CME gold futures contract data we now proceed to generate daily estimates of the Roll model incorporating autocorrelated trade direction indicators. As before, we assume constant parameters for this model during any given day, although parameters can vary across days. The Bayesian estimations follow an identical approach to simulation as described in section 4.2.¹² We compare results from the MLE method based on Regime Switching (RS) and our proposed extended MCMC method.

[Table 4 in here]

Table 4 presents our estimation results, and once again reveals that the MLE and Bayesian estimates are very similar. First, the average value of the differentials between the daily estimates of the coefficient values of c and σ_u are close to zero, and the maximum of the absolute differential values are minuscule (0.2×10^{-7}). We also note very small differences in the sets of transition probability estimates¹³. Second, the values of both c and σ_u remain

¹² Refer to Appendix B for more details on the inefficiency factors and the Geweke (1992) diagnostic tests. Table A.1 (the column ‘Roll (Bayesian)’) indicates that convergence criteria are achieved for the Roll model, since the effective size exceeds 1,000 and Geweke’s (1992) p-values are greater than 0.05 for all parameters.

¹³ Table A.2 provides more details.

significant across days, and the sample averages of the percentage effective half spread c , and of standard deviations σ_u , are 0.43×10^{-4} and 0.35×10^{-4} , respectively. The transition probabilities for the trade direction indicators are autocorrelated with coefficient values close to 0.7. These empirical results indicate the presence of moderately persistent trade direction indicator regimes. It is interesting to note that on the Brexit referendum day (23 June 2016), the estimate for c is 1.12×10^{-4} , which represents the largest single value in the sample, standard deviation estimate is 0.78×10^{-4} , reflecting an increase of close to 90% in comparison to the previous day. Finally, the persistence measure for the regime ($P+Q-1$) is 0.55, which is much larger than the average estimate of 0.4.

Attention is drawn to another feature of the Brexit referendum day estimates. Both the MLE and Bayesian methods generate substantially larger c estimates using the formulation of the Roll model incorporating autocorrelated q_t in comparison to those we derive from our benchmark Roll model (Table 2). One potential explanation helping to justify the relative size of these c coefficient estimates (with and without autocorrelated q_t) is apparent following consideration of the nature of the GMM estimates we obtain following Roll (1984). Specifically, consider the following moment condition we derive from the autoregressive form of the regime switching process: $q_{t+1} = (P-Q) + (P+Q-1)q_t + \varepsilon_{t+1}$.

The GMM estimates of c in this model are given by:

$$\gamma_1 = \text{cov}(\Delta p_t, \Delta p_{t-1}) = E[c\Delta q_t + u_t][c\Delta q_{t-1} + u_{t-1}] = c^2 E[\Delta q_t \Delta q_{t-1}] = c^2 \left((P-Q)^2 - (1-P-Q+1)^2 \right)$$

implying:

$$c = \sqrt{\frac{-\gamma_1}{(1-P-Q+1)^2 - (P-Q)^2}}$$

As the Roll model assumes $P=Q=0.5$, the resulting GMM estimate of c is:

$$c = \sqrt{-r_1} = \sqrt{-\text{cov}(\Delta p_t, \Delta p_{t-1})}.$$

The critical point to note is that once we account for autocorrelation in the trade direction indicators, the transition probabilities for both buy and sell orders enter into the determination of the value of c . From the formula, the fact we experience much more persistent regimes on

the Brexit referendum day justifies the substantially larger (log) half-spread estimates we obtain for c .

4.5 The extended Glosten and Harris model with autocorrelated q_t : a simulation exercise

We are now in a position to apply our proposed estimation procedures in an asymmetric information setting which allows for informed trading activity to have a permanent impact on the efficient price. Our model incorporates an adverse selection cost component of the effective bid-ask spread which in the present specification is a function of the square root of the signed trade volume $q_t \sqrt{V_t}$ ¹⁴. This reflects existing evidence that larger orders are more likely to contain information which has a permanent effect on the efficient price. Moreover, our estimates of the asymmetric information model assume latent and autocorrelated trade direction indicators, so only innovations in q_t impact the efficient price. This differs from the Hasbrouck (2004) formulation which incorporates independent q_t , implying the entire signed order flow impacts the efficient price.

Once again, to facilitate explanations and to clarify notation, we re-state this model:

$$p_t = m_t + cq_t, \quad m_t = m_{t-1} + (\lambda_0 + \lambda_1 \sqrt{V_t})(q_t - E_{t-1}q_t) + u_t, \quad u_t \sim N(0, \sigma_u^2)$$

where q_t is a regime switching variable with $q_t \in \{-1, +1\}$ and

$$\Pr[q_t = 1 | q_{t-1} = 1] = P, \quad \Pr[q_t = -1 | q_{t-1} = -1] = Q$$

We validate the computational integrity of our estimation algorithms, and undertake a comparison of the results from our proposed estimation method using simulations. As before, to establish a sound basis for a plausible data generating process in the simulations, we generate the data using the sample period averages of the parameter estimates we report in Table 6 assuming autocorrelation and regime persistence in the trade direction indicators. And we use the trading volume data on June 29 in simulation. To minimize simulation errors, we generate the data 50 times, and estimate the model parameters and trade direction indicators for data sample we generate and compute the simulated sample averages. We then

¹⁴ We incorporate the square root of trading volume following Hasbrouck (2004). The estimated relation between order size and price impact is then concave.

compare the estimation results obtained from MLE methods with the Bayesian MCMC methods we propose.

[Table 5 in here]

Table 5 presents the results from this simulation. Here σ_u is the estimate of the standard deviation of changes in the (log) efficient price and c is that of the order processing component of the (log) half spread; λ_0 and λ_1 are the fixed and variable permanent price impact costs, respectively. Finally, P and Q are the transition probabilities of the latent regime switching process for trade direction indicators. The “Bayesian” results are those we obtain from the Bayesian Tailored Random-walk Metropolis-Hastings Gibbs sampler in which the trade direction indicators are both conditionally simulated and autocorrelated. We generate results using 12,000 sweeps of the sampler, discarding the first 2,000. We obtain the alternative “MLE” estimates using classical MLE method to estimate the regime switching models. Once more we find that both methods provide accurate estimates of the true parameter values we use in the simulations.

4.6 The extended Glosten and Harris model with autocorrelated q_t : gold futures contract estimation

Following confirmation of the integrity of the selected estimation methodology on the basis of the simulations in section 4.5, we proceed to obtain daily estimates of the GH model with autocorrelated trade direction indicators using the gold futures data. As before, the assumption is that the parameters of this model are constant during the day may change across days. The Bayesian estimations follow an identical approach to simulation as described in section 4.2¹⁵. We compare the following two methods: the MLE incorporating regime switching (RS) and our extended MCMC approach.

Prior to a detailed discussion of the empirical results, we report the results of a model comparison among three models: the Roll model, the extended Roll model, and the extended GH model. Specifically, we compute:

¹⁵ Table A.1 (the column ‘GH (Bayesian)’) indicates that we achieve the convergence criteria for the GH model since the effective size is greater than 1,000 and Geweke’s (1992) p-values exceed 0.05 for all parameters

$$-2 \ln \left(\frac{\hat{L}_R}{\hat{L}_U} \right) \sim \chi_k^2$$

where \hat{L}_R and \hat{L}_U are the likelihood values under the restricted and unrestricted model, so in comparing the Roll model with the extended GH model, \hat{L}_R and \hat{L}_U are the likelihood values under the Roll and the extended GH model, respectively. As we impose parameter restrictions on P, Q, λ_0 , and λ_1 in the extended GH model to obtain the Roll model, the test statistics follows a chi-square distribution with 4 degrees of freedom. We consistently reject the Roll model and the extended Roll model in favour of the extended GH model for each day in our sample¹⁶.

[Table 6 in here]

In table 6 we present the estimation results from the extended GH model, which again reveal that the MLE estimates and Bayesian estimates align closely in magnitude. The difference between the daily estimates of c and σ_u we obtain from both methods exhibits an average value close to zero, and the maximum of the absolute differential value is also minuscule (0.12×10^{-4}). Other parameter values also exhibit very small differences,¹⁷ leading us to conclude that both methods provide the very similar estimates. Moreover, the results reveal a consistent pattern in relation to those we obtain from the Roll and extended Roll models. The estimates of the effective trading cost parameter, c , with a value of 0.29×10^{-4} are significant and comparable to the corresponding estimates from the Roll model, albeit somewhat lower than those from the extended Roll model. The daily estimates of the standard deviation of changes in the (log) efficient price, σ_u , are also significant, with an average value of 0.33×10^{-4} . The transition probability estimates again closely approximate those from the extended Roll model, again indicating the presence of moderately persistent regimes for the trade direction indicator.

¹⁶ Table A.3 reports detailed results on the model comparison among these three models.

¹⁷ Table A.2 provides more details on this.

Our attention is drawn to two particularly noteworthy features of the parameter estimates. First, on Brexit referendum day 23 June, the relevant estimate for c is 0.84×10^{-4} , which is the largest value in the sample, and that for σ_u is 0.78×10^{-4} , an increase of more than 250% in comparison to the previous day's. Moreover, the regime persistence coefficient, $(P+Q-1)$ is 0.5, which is significantly in excess of the average estimate, 0.4. Second, although the daily λ_0 estimates are statistically significant in only around 50% of the time, those for the slope of the price impact function arising from the effect of asymmetric information, the Kyle's lambda (λ_1) parameter are positive and always statistically significant.¹⁸ The empirical results corroborate the implications that private, fundamental-relevant information is conveyed through trading decisions and the adverse selection costs per transaction are increasing in trade size. We further discuss the economic significance of these results in terms of the decomposition of the effective spread in section 4.8.

[Table 7 in here]

Prior to further analysis of the trade classification indicator, we pause to undertake some additional analysis, of the extended GH model. We motivate this on the basis of the extreme values we observe for the transition probability estimates on two dates, namely 0.9789 and 0.9278 on 19th June and 23rd June, respectively. In comparison to the remaining (sell-side) transition probability estimates we obtain, these parameter values appear as potentially implausible outliers. We conjecture that this may relate to our assumption that the model parameters remain constant throughout the day. As the above dates lie in very close proximity to the Brexit referendum, it may be implausible to impose such a restrictive assumption on the parameters. To mitigate any concerns over model misspecification, we re-estimate the extended GH model on the 19th and 23rd June using MLE methods after dividing each of these days into 10,000 trade intervals, with the resulting estimates given in Table 7. Overall, we find that the parameter estimates exhibit significant intraday variation on these two dates, with (sell-side) transition probabilities ranging from 0.6812 to 0.9756 on 19th June and 0.668 to 0.9656 on 23rd June, respectively. As such, we conclude that the initial estimates we provide in Table 6 may indeed reflect model misspecification, arising from the assumption of

¹⁸ For an illustration see Figure 2.

constant daily parameter values.

Specifically, panel A of Table 7 reports the empirical results for 19th June. A significant change in market sentiment occurs early in the trading session on 19th June 19, after the publication of an influential survey favoring the outcome of the U.K. voting to remain in the EU. A reduction in market anxiety over a Brexit initiates an initial sell-off in safe haven assets, including gold in the early trades, and this trading behavior appears to be manifest in the estimates of two parameters in particular. First, in a much higher value for the transaction cost parameter ($c = 6.469$), and second in that capturing the persistence of the transition probability of sell orders ($Q = 0.995$) relative to that of buy orders ($P = 0.778$) in the first 10,000 trades. After the first 10,000 trades, overall trading activity within subsequent 10,000 trade buckets appears relatively balanced, with similar P and Q parameter estimates and a much smaller c , albeit the c estimate for trades in the 30,000 to 40,000 interval is also higher. We conclude that the extreme differences in the transition probabilities reported in Table 6 seem to mainly reflect the impact of the first 10,000 trades.

Panel B of Table 7 reports the empirical results for 23rd June, the day of the Brexit referendum. The time varying nature of the transition probability estimates over each 10,000 trade interval throughout this day clearly reveals the uncertainty relating to the outcome of the voting process. Initially, selling pressure in gold futures appears much higher with the first half of the trading day generating a very high persistence in the transition probability of sell orders. In contrast, gold futures buying pressure appears to be manifest during the second half of the trading day with the transition probability of buy orders evidencing more persistence. This structural break in the transition probability, combined with the fact that gold prices increase in uncertain times, captures the dynamics of the information flow relating to the Brexit vote result. We attribute the extreme differences in the two transition probabilities we report in table 6 to this structural break in the trading process.

To mitigate the effect of the early trading distortions on parameter estimates evident in panel A and the structural break in panel B of table 7, we decide to use the relatively moderate average estimates in the analyses of trade classification and the economic decomposition of the bid-ask spread we conduct in the next section..

4.7 Classification of trades for buy-sell indicator: the extended GH model

Easley, Lopez de Prado, O’Hara (2016) propose a new conceptual framework for classifying trades. They adopt the perspective of a Bayesian statistician who has priors regarding the status of the unobservable information (e.g., q_t), and is trying to extract investors underlying trading intentions from observable trade data. Our claim is that the empirical market microstructure models we use in this paper can provide plausible approximations to the Bayesian trade classification approach which constitutes their ideal. In particular, we maintain that we may interpret the Markov switching process in the Roll or GH models as the underlying process governing the evolution of the unobservable variables q_t , and the measurement equations as a plausible data generating process for the observed data relating to q_t . Thus, we can use estimates of the autocorrelated trade direction indicators, q_t , as our model-consistent trade classification algorithm.

In order to provide appropriate benchmarks with which to compare our results on the classified trades, we proceed to classify trades using the standard Tick rule¹⁹ and generate daily correlation estimates of classified trades using the Tick rule and our model consistent rules. Specifically, on the basis of the Roll and extended GH models, using Kim (1994)’s smoothing methods and MLE parameter estimates, we calculate whether each trade is initiated by buyer ($q_t = 1$) or seller ($q_t = -1$).²⁰

[Table 8 in here]

Table 8 presents the daily correlation estimates of trade classifications using the Tick rule, the Roll model, and the extended GH model. Two features are noteworthy. First, the daily correlation between the Tick rule and the Roll model (labelled Roll) estimates are almost always above 0.99, indicating that the Roll model essentially classifies trades on the basis of up- or down-ticks, as in the Tick rule. Second, while the daily correlation of the Tick rule

¹⁹ The tick rule classification uses movements in trade prices to classify a trade as either a buy or a sell. Specifically, if the transaction is above (below) the previous price, then it is a buy (sell). If there is no price change, but the previous tick change was up (down), then the trade is classified as a buy (sell).

²⁰ As both Bayesian and MLE methods produce almost identical results, we report only the latter. The Bayesian results are available on request. Appendix D discusses Kim’s (1994) smoothing algorithms.

and extended GH model (labelled GH) estimates are also high on the majority of days, they are significantly lower on both the 19th June and 23rd June, namely 0.61 and 0.45, respectively.

We conjecture a potential explanation for the second finding is as follows. Easley, Lopez de Prado, O'Hara (2016) maintain that when the underlying data is less noisy, Tick rule classifications can be superior to other rules. However, they also show that in situations where underlying data noise is substantial or order flow is imbalanced, such as when private information motivates trading, trade classifications using the Tick rule may be unreliable. In particular, the Tick rule underestimates (overestimates) the probability of buys when the direction of order flow imbalances signals positive (negative) information. As we explain in the previous section, over the days surrounding the Brexit referendum incorporate a period of great uncertainty as reflected in the results of opinion polls regarding its outcome. For example the reduction in market anxiety relating to the possibility of a leave vote on 19th June, following the release of an influential survey, initiated a major unwinding of long positions in the gold futures market in early trading, the selling pressure generating high illiquidity costs. During the remainder of this day, trades are balanced overall. This trading pattern is reflected in the daily volatility estimate, which is 0.52, much higher than its value on most other days. The day of the Brexit referendum, 23rd June also generates an abnormally high volatility estimate of 0.78. Moreover, the transition probability estimates we obtain from the extended GH model also indicate a structural break in the trading process on this day. There is initial selling pressure as the consensus in overnight opinion polls indicates a remain outcome, but the buying pressure dominates in the latter part of trading after the Brexit vote result, consistent with evidence documenting that gold prices rise during times of economic uncertainty (Erb and Harvey (2013)). The value of Kyle's lambda on June 23 is 0.324, its highest value in our sample.

In summary, the model consistent trade direction classification algorithm based on the extended GH formulation generates very similar results to the Tick rule during normal trading periods, but in periods characterised by higher uncertainty and the existence of a potentially larger price impact of trades (closely related to order imbalances), the classifications obtained from the two methods diverge significantly. As these are precisely the circumstances under which Easley, Lopez de Prado, and O'Hara (2016) argue that the Tick rule appears most

problematic in classifying trades, this suggest our proposed extended GH methods may be useful in such an environment.

It is important to state that we certainly do not intend to claim that our trade classification system is in any sense superior to other rules such as the Tick and BVC rules. As Easley, Lopez de Prado, and O'Hara (2016) note, perhaps each trade classification rule manifests both strengths and weakness, depending upon market conditions and the nature of the information environment. We believe that our approach to classifying trades is particularly well-suited to situations in which researchers use a variant of state space models incorporating regime switching to model trading environments. Moreover, our approach provides easy-to-implement model-consistent trade classification algorithms using both Bayesian and Classical methods. As such, we believe they provide a useful addition to the empirical microstructure tool kit.

4.8 Components of the effective spread: the relative contribution of order processing and adverse selection costs

How important are adverse selection costs arising from information asymmetries as constituents of the effective bid-ask spread? We address this issue by computing the relative importance in spread composition of our estimated measure of non-informational (order processing) costs and informational asymmetry components in spread composition. To facilitate the ensuing explanation, consider the log bid-ask spread implied by our model, namely:

$$\begin{aligned} p_t &= m_t + cq_t, m_t = m_{t-1} + (\lambda_0 + \lambda_1 \sqrt{V_t})(q_t - E_{t-1}q_t) + u_t \\ \Rightarrow p_t &= m_{t-1} + (\lambda_0 + \lambda_1 \sqrt{V_t})q_t + cq_t + u_t - (\lambda_0 + \lambda_1 \sqrt{V_t})(\mu + \rho q_{t-1}) \end{aligned}$$

It follows that we can express the ask (a_t) and bid (b_t) prices in our model as:

$$\begin{aligned} a_t &= m_{t-1} + (\lambda_0 + \lambda_1 \sqrt{V_t}) + c + u_t - (\lambda_0 + \lambda_1 \sqrt{V_t})(\mu + \rho q_{t-1}) \\ b_t &= m_{t-1} - (\lambda_0 + \lambda_1 \sqrt{V_t}) - c + u_t - (\lambda_0 + \lambda_1 \sqrt{V_t})(\mu + \rho q_{t-1}) \\ a_t - b_t &= 2(c + \lambda_0 + \lambda_1 \sqrt{V_t}) \end{aligned}$$

[Table 9 in here]

Based on this representation of the ask and bid prices, Table 9 and Figure 3 provide the daily estimates of transaction costs for a trade measured in ticks, $S_{GH,cs}$. We calculate this as

$S_{GH,cs} = sp_{GH,cs} \times \bar{P}$ where $sp_{GH,cs}$ is the log spread estimate ($a_t - b_t$ in the above model) with the daily average volume (\bar{V}_t) (computed as $sp_{GH,cs} = 2 \times (c + \lambda_0 + \lambda_1 \sqrt{\bar{V}_t})$), and \bar{P} is the daily average price in ticks. We also present the log spread and the daily average price in ticks in the table. For example, $S_{GH,cs}$ on 1 May is 1.1970 (i.e., $2 \times (0.4615 \times 10^{-4}) \times (1,296.9/0.1)$) where 1,296.9 is the mean of the daily prices and 0.1 is the tick size on that day.

To summarise our findings, the daily estimates of transaction costs for a trade are in the region of 1.2 ticks, reflecting the high liquidity of the gold futures markets. However, there are two exceptions to these estimates on 19 and 23 June. On these two days, the daily estimates of transaction costs for a trade are significantly higher, namely 6.265 (3.299) ticks on June 19 (June 23), respectively. This reflects the illiquidity arising from the enhanced uncertainty in the trading environment. Based on the parameter estimates from Table 6, in the final two columns of table 9 present the contribution of information and non-information related components to the spread (for an illustration see Figure 4). Specifically, the proportion of the spread attributable to the order processing cost component is $TC = c_0 / (c_0 + (\lambda_0 + \lambda_1 \sqrt{V_t}))$, and the proportion arising from adverse selection costs, the information asymmetry component, is $IC = (\lambda_0 + \lambda_1 \sqrt{V_t}) / (c_0 + (\lambda_0 + \lambda_1 \sqrt{V_t}))$. These two components are calculated by including the estimate of λ_0 only when it is statistically significant. In summary, the proportion of effective trading costs arising from non-information related components are higher than those from the information components on all days. In most cases, the former lies in the range from 55% to 70%. The exception is on June 19 where the proportion attributable to the non-information components increases to 90%. However, in general, the proportion contributed by the information related components in the gold futures market is sizeable and significant. The extended Glosten-Harris type models we estimate identify permanent price impacts arising from asymmetric information as movements in the efficient price, which is ultimately reflected in transaction prices. Viewed from this perspective, given

the nature of the gold futures market, it is perhaps not too surprising that 35 to 50% of the average bid-ask spreads reflects a compensation for bearing adverse selection risk.

5. CONCLUSION

Generating accurate measures of liquidity, and measuring trading costs and the price impact of trades is difficult when an absence of quotes makes classifying investor's trading intentions problematic. Existing literature incorporates several proposed resolutions to this problem but the dynamic evolution of trading mechanisms and the advent of electronic platforms creates further difficulties for some of these approaches. For example, Easley, Lopez de Prado and O'Hara (2016) maintain that in electronic limit order markets, often manifesting order cancellation rates of 98% or more, trade classification algorithms based on proximity to bid and ask quotes are severely compromised.

To overcome these data limitation, Hasbrouck (2004) proposes a new Bayesian approach by assuming an i.i.d. normal distribution for price innovations and latent independent trade indicators. Subsequently, Van der Wel, Menkveld, and Sarkar (2009) develop the equivalent classical maximum likelihood estimation (MLE) methods by mapping the Roll model onto Kim and Nelson's (1999) regime switching state space model. The first contribution of this paper is to develop easy-to-implement Bayesian and MLE estimators by extending both Hasbrouck (2004) and Van der Wel, Menkveld, and Sarkar (2009) to simultaneously accommodate several of the features which are omitted from these models, namely unbalanced and autocorrelated order flow and informational asymmetries. These omissions are evaluated in Chen, Linton, Schneeberger, and Yi (2016), but the present paper is the first to undertake a comprehensive empirical implementation which addresses these drawbacks. The second contribution of this paper is to provide robust trade direction classification mechanisms without recourse to quotes. Our proposed classification systems utilise both Bayesian MCMC methods and classical filtering and smoothing algorithms for latent trade direction indicators.

Simulation results reveal that the methods we propose are reliable. For purposes of illustration, we analyse the empirical behaviour of gold futures prices from the CME contract during a period of market uncertainty surrounding the UK's Brexit referendum in 2016. This

analysis reveals several noteworthy features. First, trade direction indicators appear highly autocorrelated, leading to measured bid-ask spreads being larger, in an economically meaningful sense, than those obtained from alternative estimates employing independent trade direction indicators. Second, they provide statistical support for asymmetric information models of the type proposed by Glosten and Harris (1988) in the presence of latent and autocorrelated trade direction indicators, thereby evidence that the trade impact coefficients implied by the asymmetric information model, which reflect Kyle's lambda, are important elements of liquidity. Third, they reveal that the trade classifications we obtain from the Roll model used in Hasbrouck (2004) and the Tick rule are essentially identical. Finally, our model consistent trade classification algorithm provides very similar results to the Tick rule during normal trading periods. However, in the presence of greater uncertainty when trading potentially generates a greater price impact (resulting from order flow imbalances), our trade classification indicator often diverges significantly from those using the Tick rule. Easley, Lopez de Prado, and O'Hara (2016) maintain that Tick rule classifications appear particularly problematic in periods of high volatility exhibiting imbalances in order flow. We believe the approach to trade classification we propose shows some promise in this type of trading environment. However, we certainly do not claim that our trade classification system is superior to other rules. As Easley, Lopez de Prado and O'Hara (2016) note, each trade classification rule may demonstrate both strengths and weakness, depending on the underlying market characteristics. Instead, we maintain that our approach may be best suited to classifying trades consistently in environments where a variant of state space models with regime switching yields a realistic approximation to the trading conditions. Moreover, our methods have the advantage of providing easy-to-implement model consistent trade classification algorithms using both Bayesian and Classical estimation methods. As such, we believe they may be a useful addition to the empirical microstructure tool kit.

REFERENCES

Brennan, M.J., and A. Subrahmanyam, 1996, Market Microstructure and Asset Pricing: On the Compensation for Illiquidity in Stock Returns, *Journal of Financial Economics*, 41, 441-464.

Brogaard, J., Hendershott, T., and Riordan, R., 2014. High Frequency Trading and Price Discovery. *Review of Financial Studies*, 27 (8), 2267–2306,

Chib, S., and S. Ramamurthy, 2010, Tailored Randomized Block MCMC Methods with Application to DSGE Models, *Journal of Econometrics*, 155(1), 19-38.

Chen, X., Linton, O., Schneeberger, S., and Y. Yi, 2016, Simple Nonparametric Estimators for the Bid-Ask Spread in the Roll Model, March 30, Working paper

Choi, J.Y., Salandro, D., and K. Shastri, 1988, On the Estimation of Bid-ask Spreads: Theory and Evidence, *Journal of Financial and Quantitative Analysis*, 23, 219-30.

Easley, D, López de Prado, M., and M. O'Hara, 2012, Flow Toxicity and Liquidity in a High-frequency World, *The Review of Financial Studies*, 25(5), 1457–1493

Easley, D, Lopez de Prado, M., and M. O'Hara, 2016, Discerning Information from Trade Data, *Journal of Financial Economics*, 120(2), 269-285.

Erb, C.B., and C. R. Harvey, 2013, the Golden Dilemma, NBER working paper.

Foucault, T., Pagano, M., and A. Röell, 2013, Market Liquidity: Theory, Evidence, and Policy, Oxford University Press.

Geweke, J., 1992, Evaluating the Accuracy of Sampling-based Approaches to the Calculation of Posterior Moments, *Bayesian Statistics 4*, Oxford University Press.

Glosten, L.R., and L.E. Harris, 1988, Estimating the Components of the Bid-ask Spread, *Journal of Financial Economics*, 21, 123–142.

Glosten, L. R., and P. Milgrom, 1985, Bid, Ask and Transaction Prices in a Specialist Market with Heterogeneously Informed Traders, *Journal of Financial Economics*, 14, 71-100.

Hasbrouck, J, 1991, Measuring the Information Content of Stock Trades, *Journal of Finance*, 46, 179-207.

Hasbrouck, J, 2004, Liquidity in the Futures Pit: Inferring Market Dynamics from Incomplete Data, *Journal of Financial and Quantitative Analysis*, 39, 305–326.

Hasbrouck, J., 2007, Empirical Market Microstructure, Oxford University Press.

Hauptfleisch, M., Putniñš, T.J., and B. Lucey, 2016, Who Sets the Price of Gold? London or New York, *Journal of Futures Markets*, 36(6), 564-586.

Hendershott, T., and A. J. Menkveld, 2014, Price Pressures, *Journal of Financial Economics*, 114, 405-423.

Holden, C W., and S. Jacobsen., 2014, Liquidity Measurement Problems in Fast, Competitive Markets: Expensive and Cheap Solutions, *Journal of Finance*, 69(4), 1747-1785.

Holden, C. W., Jacobsen, S.E., and A. Subrahmanyam, 2013, The Empirical Analysis of Liquidity, *Foundations and Trends in Finance*, 8(4), 263-365.

Kim, C. J., 1994, Dynamic Linear Models with Markov-switching, *Journal of Econometrics*, 60,1-22.

Kim, C. J., and C. R. Nelson, 1999, State-space Models with Regime Switching: Classical and Gibbs-sampling Approaches with Applications, MIT Press.

Kim, S., Shephard, N., and S. Chib, 1998, Stochastic volatility: Likelihood inference and comparison with ARCH models. *Review of Economic Studies*, 65, 361–393.

Kyle, A., 1985, Continuous Auctions and Insider Trading, *Econometrica*, 53, 1315-1336.

Labuszewsk, J.W., Nyhoff, J.E., Co, R., and P. E. Peterson, 2010, The CME group risk management handbook, John Wiley & Sons.

Lee, C.M.C., and M. J. Ready, 1991, Inferring Trade Direction from Intraday Data, *Journal of Finance*, 46, 733-46.

Madhavan, A., Richardson, M., and M. Roomans, 1997, Why Do Security Prices Change?

Review of Financial Studies, 10, 1035-64.

Marshall, B.R., Nguyen, N.H., and N. Visaltanachoti, 2013, Liquidity Commonality in Commodities, 37 (1), *Journal of Banking and Finance*, 11-20.

Menkveld, A.J., Koopman, S.J., Lucas, A., 2007. Modelling Round-the-clock Price Discovery for Crosslisted Stocks Using State Space Methods. *Journal of Business and Economic Statistics* 25, 213–225.

Menkveld, A.J., 2013. High-frequency Trading and the New Market Makers. *Journal of Financial Markets* 16, 712–740.

Panayides M., Shohfi, T., and J. Smith, 2014, Comparing Trade Flow Classification Algorithms in the Electronic Era: The Good, the Bad, and the Uninformative, September, Working paper.

Roll, R., 1984, A Simple Implicit Measure of the Effective Bid-ask Spread in an Efficient Market, *Journal of Finance*, 39(4), 1127-1139.

Sadka, R., 2006, Momentum and Post Earnings Announcement Drift Anomalies: the Role of Liquidity risk, *Journal of Financial Economics*, 80, 309-349.

Van der Wel, M., Menkveld, A. J. and A. Sarkar, 2009, Are Market Makers Uninformed and Passive? Signing Trades in the Absence of Quotes, Federal Reserve Bank of New York, Staff Reports, no.395, September.

Table 1. Contract Descriptions and Summary Sample Statistics

Contract	Gold futures
Expiration months	June, 2016 (GCM6) and August, 2016 (GCQ6)
Trading sample months	May, 2016 - June, 2016
Numbers of trading days	44
Avg. price	1269.0
Price units	U.S. dollars and cents per troy ounce
Tick	\$0.10 per troy ounce
Avg. tick/price	0.008%
Size of contract	100 troy ounce
Avg. dollar value	\$126,900.00
Std. Dev. Of price change (log price X 10,000)	0.5579
Std. Dev. Of price change (ticks)	7.0849
Avg. daily trades	58,205
Avg. time between trades (seconds)	1.618808

Table 2. The Roll Model: MLE and Bayesian Methods

$$p_t = m_t + cq_t, m_t = m_{t-1} + u_t, u_t \sim N(0, \sigma_u^2), q_t \in \{-1, 1\} \text{ where } \Pr[q_t = 1 | q_{t-1} = 1] = \Pr[q_t = -1 | q_{t-1} = -1] = 0.5$$

This table provides daily parameter estimates of the above model for the gold futures contract traded on the CME Globex electronic trading platform from May 1, 2016 to June 30, 2016. Electronic trading on CME Globex is available virtually 24 hours a day from Sunday 6:00 p.m. through Friday 5:00 p.m. EST, with a 60-minute break each day beginning at 5:00 p.m. EST. Thus, we assume the trading activity on any given date starts at 6:00 p.m. and finishes at 5:00 p.m. EST next day. For example, the May 1 trading starts at 6:00 p.m. on May 1 and finishes at 5:00 p.m. on May 2. σ_u is the standard deviation of the log efficient price changes, and c is the (log) half spread. Estimates labelled “Roll(Bayesian)” are Hasbrouck (2004)’s Gibbs sampler estimates in which trade direction indicators are conditionally simulated. Estimates labelled “Roll(MLE)” are MLE estimates based on the Roll model. In this table, 10,000 fold of c and σ_u estimates are reported. And to guarantee a correct statistical inference, we start all Bayesian estimations with 100,000 burn-in period and 250,000 total numbers of iterations and increase these numbers by 10,000 until the convergence criteria for the inefficiency factors and the Geweke (1992)’s diagnostic tests are satisfied simultaneously for all parameters.

Date	Parameters	Roll (MLE)		Roll (Bayesian)	
		$c \times 10,000$	$\sigma_u \times 10,000$	$c \times 10,000$	$\sigma_u \times 10,000$
1-May	Mean	0.2108	0.4510	0.2107	0.4510
	Std	[0.0023]	[0.0026]	[0.0026]	[0.0023]
2-May	Mean	0.2441	0.4346	0.2442	0.4346
	Std	[0.0024]	[0.0027]	[0.0025]	[0.0024]
3-May	Mean	0.2273	0.4511	0.2273	0.4511
	Std	[0.0023]	[0.0025]	[0.0025]	[0.0023]
4-May	Mean	0.2237	0.4433	0.2237	0.4434
	Std	[0.0025]	[0.0028]	[0.0027]	[0.0025]
5-May	Mean	0.2181	0.4674	0.2181	0.4675
	Std	[0.0021]	[0.0023]	[0.0023]	[0.0021]
8-May	Mean	0.2112	0.4271	0.2113	0.4270
	Std	[0.0024]	[0.0026]	[0.0025]	[0.0023]
9-May	Mean	0.2135	0.4363	0.2135	0.4363
	Std	[0.0026]	[0.0028]	[0.0028]	[0.0025]
10-May	Mean	0.2421	0.4113	0.2421	0.4114
	Std	[0.0029]	[0.0032]	[0.0031]	[0.0030]
11-May	Mean	0.2390	0.4274	0.2390	0.4273
	Std	[0.0026]	[0.0029]	[0.0027]	[0.0026]
12-May	Mean	0.2302	0.4392	0.2302	0.4392
	Std	[0.0026]	[0.0029]	[0.0028]	[0.0026]
15-May	Mean	0.3073	0.3688	0.3061	0.3702
	Std	[0.0033]	[0.0043]	[0.0062]	[0.0063]
16-May	Mean	0.2505	0.4147	0.2506	0.4147
	Std	[0.0027]	[0.0031]	[0.0029]	[0.0028]
17-May	Mean	0.2463	0.4616	0.2463	0.4616
	Std	[0.0024]	[0.0026]	[0.0025]	[0.0024]
18-May	Mean	0.2614	0.4127	0.2616	0.4125
	Std	[0.0029]	[0.0032]	[0.0032]	[0.0031]
19-May	Mean	0.2632	0.3982	0.2637	0.3977
	Std	[0.0039]	[0.0044]	[0.0048]	[0.0047]
22-May	Mean	0.2403	0.3942	0.2407	0.3939
	Std	[0.0038]	[0.0041]	[0.0041]	[0.0038]
23-May	Mean	0.3548	0.3062	0.3547	0.3062

	Std	[0.0016]	[0.0024]	[0.0013]	[0.0011]
24-May	Mean	0.3463	0.3071	0.3463	0.3072
	Std	[0.0017]	[0.0027]	[0.0015]	[0.0013]
25-May	Mean	0.2304	0.4424	0.2304	0.4423
	Std	[0.0031]	[0.0033]	[0.0033]	[0.0030]
26-May	Mean	0.2503	0.4331	0.2503	0.4330
	Std	[0.0032]	[0.0035]	[0.0033]	[0.0032]
29-May	Mean	0.2765	0.4867	0.2766	0.4867
	Std	[0.0037]	[0.0043]	[0.0040]	[0.0039]
30-May	Mean	0.3359	0.3473	0.3356	0.3476
	Std	[0.0026]	[0.0039]	[0.0026]	[0.0026]
31-May	Mean	0.3553	0.3256	0.3553	0.3257
	Std	[0.0018]	[0.0029]	[0.0016]	[0.0015]
1-Jun	Mean	0.2734	0.4109	0.2739	0.4105
	Std	[0.0041]	[0.0047]	[0.0052]	[0.0051]
2-Jun	Mean	0.2425	0.5173	0.2425	0.5173
	Std	[0.0024]	[0.0026]	[0.0026]	[0.0024]
5-Jun	Mean	0.2398	0.4202	0.2398	0.4202
	Std	[0.0031]	[0.0033]	[0.0031]	[0.0029]
6-Jun	Mean	0.3456	0.3020	0.3455	0.3020
	Std	[0.0018]	[0.0029]	[0.0016]	[0.0014]
7-Jun	Mean	0.3400	0.2914	0.3400	0.2914
	Std	[0.0016]	[0.0026]	[0.0014]	[0.0012]
8-Jun	Mean	0.3304	0.3001	0.3304	0.3002
	Std	[0.0017]	[0.0028]	[0.0015]	[0.0014]
9-Jun	Mean	0.3227	0.3074	0.3226	0.3075
	Std	[0.0019]	[0.0030]	[0.0018]	[0.0016]
12-Jun	Mean	0.2350	0.4005	0.2352	0.4004
	Std	[0.0027]	[0.0030]	[0.0029]	[0.0027]
13-Jun	Mean	0.3273	0.2840	0.3273	0.2841
	Std	[0.0014]	[0.0023]	[0.0012]	[0.0011]
14-Jun	Mean	0.2248	0.4496	0.2248	0.4496
	Std	[0.0024]	[0.0027]	[0.0026]	[0.0024]
15-Jun	Mean	0.2463	0.4026	0.2464	0.4025
	Std	[0.0022]	[0.0024]	[0.0023]	[0.0022]
16-Jun	Mean	0.2374	0.3886	0.2375	0.3885
	Std	[0.0029]	[0.0032]	[0.0030]	[0.0029]
19-Jun	Mean	0.1846	0.5301	0.1845	0.5302
	Std	[0.0026]	[0.0026]	[0.0031]	[0.0024]
20-Jun	Mean	0.2169	0.4635	0.2169	0.4635
	Std	[0.0024]	[0.0026]	[0.0027]	[0.0024]
21-Jun	Mean	0.2151	0.4446	0.2151	0.4446
	Std	[0.0028]	[0.0031]	[0.0031]	[0.0028]
22-Jun	Mean	0.2087	0.5066	0.2087	0.5066
	Std	[0.0027]	[0.0029]	[0.0032]	[0.0027]
23-Jun	Mean	0.3313	0.9604	0.3312	0.9604
	Std	[0.0027]	[0.0025]	[0.0030]	[0.0023]
26-Jun	Mean	0.2081	0.5356	0.2081	0.5356
	Std	[0.0022]	[0.0023]	[0.0026]	[0.0021]
27-Jun	Mean	0.2396	0.4474	0.2396	0.4474
	Std	[0.0025]	[0.0028]	0.0027	0.0026
28-Jun	Mean	0.2280	0.4369	0.2280	0.4369
	Std	[0.0025]	[0.0028]	0.0027	0.0025
29-Jun	Mean	0.2231	0.4189	0.2230	0.4189
	Std	[0.0025]	[0.0028]	0.0026	0.0024
Average	Mean	0.2591	0.4252	0.2591	0.4251

Table 3. The extended Roll Model (MS) : Simulation Study I

$$p_t = m_t + cq_t, m_t = m_{t-1} + u_t, u_t \sim N(0, \sigma_u^2), q_t \in \{-1, 1\} \text{ where } \Pr[q_t = 1 | q_{t-1} = 1] = P, \Pr[q_t = -1 | q_{t-1} = -1] = Q$$

This table provides parameter estimates of the above model using simulated data. In order to establish a sound basis for a plausible data generating process in the simulations, we generate the data using the averages of parameter estimates (labelled as TRUE) reported in Table 4.

σ_u is the standard deviation of the (log) efficient price changes: c is the (log) half spread. P and Q are transition probabilities. Estimates labeled “MS (Bayesian)” are our single-move Gibbs sampler estimates in which trade direction indicators are conditionally simulated and autocorrelated. Estimates labelled “MS (MLE)” are MLE estimates based on the extended Roll model. To minimize simulation errors, we simulate data 50 times, and estimate the parameters and trade direction indicators of these models for each generated data sample and compute simulated sample averages of c , σ_u , P and Q . In this table, 10,000 fold of c and σ_u estimates are reported.

Model	Parameters	TRUE	MS (MLE)		MS (Bayesian)	
		Average estimate	Estimate	STD	Estimate	STD
MS	$c \times 10,000$	0.43	0.4297	0.0021	0.4297	0.0019
	$\sigma_u \times 10,000$	0.35	0.3498	0.0025	0.3499	0.0014
	P	0.70	0.6990	0.0043	0.6991	0.0042
	Q	0.72	0.7193	0.0041	0.7194	0.0039

Table 4. The extended Roll Model (MS) : MLE and Bayesian Methods

$$p_t = m_t + cq_t, m_t = m_{t-1} + u_t, u_t \sim N(0, \sigma_u^2), q_t \in \{-1, 1\} \text{ where } \Pr[q_t = 1 | q_{t-1} = 1] = P, \Pr[q_t = -1 | q_{t-1} = -1] = Q$$

This table provides daily parameter estimates of the above model for the gold futures contract traded on the CME Globex electronic trading platform from May 1, 2016 to June 30, 2016. (See the caption of Table 2 for further details on the dating convention used in the paper) σ_u is the standard deviation of the (log) efficient price changes: c is the (log) half spread. P and Q are transition probabilities. Estimates labeled “MS (Bayesian)” are our single-move Gibbs sampler estimates in which trade direction indicators are conditionally simulated and autocorrelated. Estimates labelled “MS (MLE)” are MLE estimates based on the extended Roll model. In this table 10,000 fold of c and σ_u estimates are reported. And to guarantee a correct statistical inference, we start all Bayesian estimations with 100,000 burn-in period and 250,000 total numbers of iterations and increase these numbers by 10,000 until the convergence criteria for the inefficiency factors and the Geweke(1992)’s diagnostic tests are satisfied simultaneously for all parameters.

Date	Parameters	MS(MLE)				MS(Bayesian)			
		$c \times 10,000$	$\sigma_u \times 10,000$	P	Q	$c \times 10,000$	$\sigma_u \times 10,000$	P	Q
1-May	Mean	0.3823	0.3565	0.7128	0.7241	0.3823	0.3566	0.7129	0.7240
	Std	[0.0021]	[0.0027]	[0.0058]	[0.0058]	[0.0021]	[0.0016]	[0.0058]	[0.0055]
2-May	Mean	0.3874	0.3481	0.6848	0.7000	0.3875	0.3481	0.6848	0.7002
	Std	[0.0018]	[0.0025]	[0.0054]	[0.0052]	[0.0018]	[0.0013]	[0.0053]	[0.0050]
3-May	Mean	0.3999	0.3492	0.7106	0.7153	0.3999	0.3493	0.7103	0.7158
	Std	[0.0018]	[0.0025]	[0.0054]	[0.0054]	[0.0018]	[0.0013]	[0.0053]	[0.0052]
4-May	Mean	0.3900	0.3463	0.7127	0.7102	0.3900	0.3464	0.7129	0.7102
	Std	[0.0020]	[0.0027]	[0.0053]	[0.0054]	[0.0020]	[0.0014]	[0.0052]	[0.0053]
5-May	Mean	0.4024	0.3631	0.7139	0.7271	0.4024	0.3632	0.7136	0.7275
	Std	[0.0018]	[0.0025]	[0.0055]	[0.0055]	[0.0018]	[0.0014]	[0.0056]	[0.0052]
8-May	Mean	0.3886	0.3241	0.7057	0.7441	0.3887	0.3241	0.7058	0.7440
	Std	[0.0018]	[0.0025]	[0.0050]	[0.0045]	[0.0018]	[0.0011]	[0.0051]	[0.0043]
9-May	Mean	0.3856	0.3390	0.7247	0.7183	0.3856	0.3390	0.7246	0.7185
	Std	[0.0021]	[0.0028]	[0.0055]	[0.0056]	[0.0021]	[0.0014]	[0.0054]	[0.0054]
10-May	Mean	0.3850	0.3266	0.7052	0.7006	0.3850	0.3266	0.7053	0.7007
	Std	[0.0019]	[0.0026]	[0.0052]	[0.0053]	[0.0019]	[0.0012]	[0.0052]	[0.0053]
11-May	Mean	0.3883	0.3365	0.6897	0.7090	0.3883	0.3365	0.6901	0.7088
	Std	[0.0018]	[0.0026]	[0.0052]	[0.0050]	[0.0018]	[0.0013]	[0.0052]	[0.0049]
12-May	Mean	0.3891	0.3449	0.6928	0.7181	0.3891	0.3450	0.6929	0.7180
	Std	[0.0020]	[0.0027]	[0.0055]	[0.0051]	[0.0020]	[0.0014]	[0.0055]	[0.0049]
15-May	Mean	0.3909	0.3293	0.6695	0.6860	0.3910	0.3293	0.6696	0.6861
	Std	[0.0017]	[0.0025]	[0.0052]	[0.0051]	[0.0017]	[0.0012]	[0.0053]	[0.0050]
16-May	Mean	0.3850	0.3332	0.6909	0.6936	0.3850	0.3332	0.6909	0.6937
	Std	[0.0018]	[0.0025]	[0.0052]	[0.0051]	[0.0018]	[0.0012]	[0.0051]	[0.0051]
17-May	Mean	0.4002	0.3686	0.6885	0.6976	0.4002	0.3686	0.6885	0.6977
	Std	[0.0019]	[0.0025]	[0.0056]	[0.0055]	[0.0019]	[0.0015]	[0.0056]	[0.0054]
18-May	Mean	0.3996	0.3278	0.6846	0.7088	0.3997	0.3279	0.6847	0.7089
	Std	[0.0016]	[0.0022]	[0.0045]	[0.0042]	[0.0016]	[0.0011]	[0.0045]	[0.0041]
19-May	Mean	0.3907	0.3238	0.6822	0.7107	0.3907	0.3239	0.6826	0.7106
	Std	[0.0021]	[0.0028]	[0.0057]	[0.0053]	[0.0020]	[0.0013]	[0.0057]	[0.0052]
22-May	Mean	0.3897	0.3075	0.7042	0.7312	0.3897	0.3075	0.7045	0.7309
	Std	[0.0019]	[0.0025]	[0.0054]	[0.0050]	[0.0019]	[0.0011]	[0.0054]	[0.0049]
23-May	Mean	0.4098	0.3035	0.7051	0.7187	0.4098	0.3034	0.7054	0.7186
	Std	[0.0015]	[0.0021]	[0.0048]	[0.0046]	[0.0016]	[0.0010]	[0.0047]	[0.0045]

24-May	Mean	0.4025	0.3055	0.7208	0.7053	0.4025	0.3055	0.7207	0.7054
	Std	[0.0018]	[0.0023]	[0.0049]	[0.0052]	[0.0018]	[0.0010]	[0.0049]	[0.0052]
25-May	Mean	0.4055	0.3369	0.7081	0.7255	0.4055	0.3369	0.7080	0.7257
	Std	[0.0021]	[0.0029]	[0.0056]	[0.0053]	[0.0021]	[0.0014]	[0.0055]	[0.0052]
26-May	Mean	0.4085	0.3356	0.7040	0.7075	0.4085	0.3357	0.7042	0.7074
	Std	[0.0020]	[0.0027]	[0.0052]	[0.0051]	[0.0020]	[0.0013]	[0.0052]	[0.0051]
29-May	Mean	0.4116	0.4079	0.6459	0.6978	0.4117	0.4081	0.6464	0.6979
	Std	[0.0034]	[0.0041]	[0.0098]	[0.0087]	[0.0034]	[0.0027]	[0.0096]	[0.0079]
30-May	Mean	0.4023	0.3312	0.6935	0.6882	0.4023	0.3313	0.6937	0.6881
	Std	[0.0020]	[0.0027]	[0.0052]	[0.0053]	[0.0019]	[0.0013]	[0.0052]	[0.0053]
31-May	Mean	0.4080	0.3208	0.6865	0.6933	0.4080	0.3209	0.6866	0.6933
	Std	[0.0018]	[0.0025]	[0.0050]	[0.0049]	[0.0018]	[0.0011]	[0.0049]	[0.0048]
1-Jun	Mean	0.4039	0.3362	0.6967	0.6979	0.4040	0.3362	0.6969	0.6979
	Std	[0.0023]	[0.0030]	[0.0059]	[0.0058]	[0.0022]	[0.0014]	[0.0058]	[0.0057]
2-Jun	Mean	0.7386	0.5375	0.4476	0.9773	0.7406	0.5375	0.4550	0.9774
	Std	[0.0150]	[0.0028]	[0.0206]	[0.0013]	[0.0110]	[0.0020]	[0.0175]	[0.0011]
5-Jun	Mean	0.4045	0.3204	0.7063	0.7267	0.4045	0.3204	0.7063	0.7267
	Std	[0.0018]	[0.0025]	[0.0052]	[0.0049]	[0.0018]	[0.0012]	[0.0052]	[0.0049]
6-Jun	Mean	0.3913	0.3019	0.6896	0.6881	0.3913	0.3020	0.6897	0.6882
	Std	[0.0020]	[0.0027]	[0.0057]	[0.0057]	[0.0020]	[0.0012]	[0.0056]	[0.0056]
7-Jun	Mean	0.3908	0.2921	0.7036	0.7176	0.3908	0.2921	0.7039	0.7174
	Std	[0.0017]	[0.0023]	[0.0049]	[0.0047]	[0.0017]	[0.0010]	[0.0049]	[0.0046]
8-Jun	Mean	0.3802	0.2984	0.6956	0.6994	0.3803	0.2984	0.6957	0.6995
	Std	[0.0019]	[0.0025]	[0.0051]	[0.0051]	[0.0018]	[0.0011]	[0.0050]	[0.0049]
9-Jun	Mean	0.3795	0.3019	0.7091	0.6943	0.3795	0.3019	0.7092	0.6944
	Std	[0.0019]	[0.0025]	[0.0052]	[0.0054]	[0.0018]	[0.0011]	[0.0051]	[0.0054]
12-Jun	Mean	0.3822	0.3102	0.7173	0.6964	0.3822	0.3103	0.7174	0.6963
	Std	[0.0016]	[0.0023]	[0.0046]	[0.0049]	[0.0016]	[0.0010]	[0.0045]	[0.0048]
13-Jun	Mean	0.3766	0.2848	0.7065	0.7152	0.3766	0.2848	0.7068	0.7150
	Std	[0.0016]	[0.0021]	[0.0046]	[0.0045]	[0.0016]	[0.0009]	[0.0045]	[0.0045]
14-Jun	Mean	0.4022	0.3423	0.7234	0.7054	0.4022	0.3423	0.7232	0.7057
	Std	[0.0018]	[0.0026]	[0.0059]	[0.0061]	[0.0018]	[0.0013]	[0.0059]	[0.0063]
15-Jun	Mean	0.3808	0.3154	0.6889	0.6915	0.3809	0.3154	0.6890	0.6915
	Std	[0.0012]	[0.0019]	[0.0037]	[0.0037]	[0.0012]	[0.0008]	[0.0036]	[0.0036]
16-Jun	Mean	0.3767	0.3057	0.7022	0.7132	0.3767	0.3057	0.7026	0.7129
	Std	[0.0017]	[0.0023]	[0.0048]	[0.0046]	[0.0016]	[0.0010]	[0.0048]	[0.0046]
19-Jun	Mean	0.8509	0.5325	0.6238	0.9883	0.8516	0.5325	0.6244	0.9883
	Std	[0.0146]	[0.0024]	[0.0238]	[0.0007]	[0.0133]	[0.0018]	[0.0189]	[0.0006]
20-Jun	Mean	0.3881	0.3629	0.7117	0.7022	0.3881	0.3630	0.7121	0.7020
	Std	[0.0020]	[0.0027]	[0.0058]	[0.0060]	[0.0021]	[0.0016]	[0.0056]	[0.0059]
21-Jun	Mean	0.3830	0.3463	0.7262	0.6948	0.3830	0.3464	0.7265	0.6945
	Std	[0.0023]	[0.0031]	[0.0060]	[0.0065]	[0.0023]	[0.0016]	[0.0056]	[0.0065]
22-Jun	Mean	0.3988	0.4140	0.7303	0.7289	0.3987	0.4143	0.7315	0.7280
	Std	[0.0029]	[0.0033]	[0.0098]	[0.0097]	[0.0030]	[0.0025]	[0.0096]	[0.0095]
23-Jun	Mean	1.1238	0.7851	0.5974	0.9404	1.1237	0.7851	0.5981	0.9404
	Std	[0.0047]	[0.0022]	[0.0060]	[0.0009]	[0.0043]	[0.0017]	[0.0057]	[0.0008]
26-Jun	Mean	0.6137	0.5204	0.9633	0.5514	0.6144	0.5205	0.9634	0.5527
	Std	[0.0106]	[0.0028]	[0.0018]	[0.0174]	[0.0077]	[0.0019]	[0.0015]	[0.0164]
27-Jun	Mean	0.3827	0.3605	0.6557	0.7129	0.3827	0.3606	0.6559	0.7129
	Std	[0.0020]	[0.0029]	[0.0070]	[0.0063]	[0.0021]	[0.0016]	[0.0069]	[0.0057]
28-Jun	Mean	0.3777	0.3472	0.7101	0.6823	0.3777	0.3473	0.7103	0.6822
	Std	[0.0021]	[0.0028]	[0.0062]	[0.0066]	[0.0021]	[0.0015]	[0.0059]	[0.0065]
29-Jun	Mean	0.3803	0.3251	0.7091	0.7118	0.3803	0.3252	0.7094	0.7115
	Std	[0.0018]	[0.0026]	[0.0052]	[0.0053]	[0.0018]	[0.0012]	[0.0052]	[0.0051]
Average	Mean	0.4320	0.3570	0.6966	0.7220	0.4392	0.3651	0.7011	0.7215

Table 5. The extended GH Model (GH) : Simulation Study II

$$p_t = m_t + cq_t, m_t = m_{t-1} + \lambda_t (q_t - E[q_t | \Omega_{t-1}]) + u_t, u_t \sim N(0, \sigma_u^2), q_t \in \{-1, 1\}$$

$$\text{where } \Pr[q_t = 1 | q_{t-1} = 1] = P, \Pr[q_t = -1 | q_{t-1} = -1] = Q \text{ and } \lambda_t = \lambda_0 + \lambda_1 \sqrt{V_t}$$

This table provides parameter estimates of the above model using simulated data. In order to establish a sound basis for a plausible data generating process in the simulations, we generate the data using the averages of parameter estimates (labelled as TRUE) reported in Table 6.

σ_u is the standard deviation of the (log) efficient price changes: c is the order processing component of the (log) half spread. P and Q are transition probabilities. λ_0 and λ_1 are the fixed and variable permanent price impact costs, respectively. Estimates labeled “GH (Bayesian)” are our tailored Random-walk MH sampler estimates in which trade direction indicators are conditionally simulated and autocorrelated. Estimates labelled “GH (MLE)” are MLE estimates based on the extended GH model. To minimize simulation errors, we simulate data 50 times, and estimate the parameters and trade direction indicators of these models for each generated data sample and compute simulated sample averages of $\sigma_u, c, \lambda_0, \lambda_1, P$ and Q . In this table, 10,000 fold of c, λ_0, λ_1 and σ_u estimates are reported.

Model	Parameters	Average estimate	TRUE		GH (MLE)		GH (Bayesian)	
			Estimate	STD	Estimate	STD	Estimate	STD
GH	$c \times 10,000$	0.30	0.3005	0.0032	0.3005	0.0033		
	$\sigma_u \times 10,000$	0.33	0.3299	0.0024	0.3299	0.0013		
	$\lambda_0 \times 10,000$	0.02	0.0191	0.0047	0.0191	0.0052		
	$\lambda_1 \times 10,000$	0.10	0.1000	0.0023	0.1000	0.0021		
	P	0.70	0.6995	0.0035	0.6996	0.0034		
	Q	0.71	0.7098	0.0034	0.7099	0.0033		

Table 6. The extended GH Model (GH) : Estimation using MLE and Bayesian Methods

This table provides daily parameter estimates of the above model for the gold futures contract traded on the CME Globex electronic trading platform from May 1, 2016 to June 30, 2016. (See the caption of Table 2 for further details on the dating convention used in the paper.) σ_u is the standard deviation of the (log) efficient price changes; c is the order processing component of the (log) half spread. P and Q are transition probabilities. λ_0 and λ_1 are the fixed and variable permanent price impact costs, respectively, due to adverse selection. Estimates labeled “GH (Bayesian)” are our tailored random-walk MH sampler estimates in which trade direction indicators are conditionally simulated and autocorrelated. Estimates labelled “GH (MLE)” are MLE estimates based on the extended GH model. In this table, 10,000 fold of c , λ_0 , λ_1 , and σ_u estimates are reported. And to guarantee a correct statistical inference, we start all Bayesian estimations with 100,000 burn-in period and 250,000 total numbers of iterations and increase these numbers by 10,000 until the convergence criteria for the inefficiency factors and the Geweke (1992)’s diagnostic tests are satisfied simultaneously for all parameters.

Date	Parameters	GH(MLE)						GH(Bayesian)					
		$c_{\times 10,000}$	$\sigma_{u \times 10,000}$	$\lambda_{0 \times 10,000}$	$\lambda_{1 \times 10,000}$	P	Q	$c_{\times 10,000}$	$\sigma_{u \times 10,000}$	$\lambda_{0 \times 10,000}$	$\lambda_{1 \times 10,000}$	P	Q
1-May	Mean	0.2425	0.3265	0.0409	0.1052	0.7013	0.7082	0.2426	0.3266	0.0405	0.1052	0.7017	0.7078
	Std	[0.0030]	[0.0028]	[0.0049]	[0.0025]	[0.0036]	[0.0035]	[0.0033]	[0.0014]	[0.0064]	[0.0025]	[0.0037]	[0.0037]
2-May	Mean	0.2677	0.3197	0.0102	0.1113	0.6764	0.6865	0.2677	0.3198	0.0102	0.1113	0.6765	0.6864
	Std	[0.0026]	[0.0026]	[0.0043]	[0.0021]	[0.0035]	[0.0034]	[0.0029]	[0.0013]	[0.0057]	[0.0022]	[0.0036]	[0.0034]
3-May	Mean	0.2719	0.3235	0.0289	0.1010	0.7022	0.6970	0.2719	0.3235	0.0290	0.1009	0.7021	0.6973
	Std	[0.0027]	[0.0026]	[0.0043]	[0.0022]	[0.0034]	[0.0034]	[0.0030]	[0.0012]	[0.0056]	[0.0022]	[0.0035]	[0.0035]
4-May	Mean	0.2597	0.3206	0.0437	0.0956	0.7013	0.7044	0.2598	0.3207	0.0435	0.0956	0.7013	0.7045
	Std	[0.0030]	[0.0028]	[0.0047]	[0.0022]	[0.0036]	[0.0036]	[0.0033]	[0.0013]	[0.0062]	[0.0023]	[0.0037]	[0.0037]
5-May	Mean	0.2708	0.3354	0.0207	0.1073	0.6915	0.7088	0.2708	0.3355	0.0204	0.1075	0.6920	0.7084
	Std	[0.0027]	[0.0025]	[0.0043]	[0.0022]	[0.0034]	[0.0032]	[0.0029]	[0.0013]	[0.0055]	[0.0022]	[0.0034]	[0.0033]
8-May	Mean	0.2611	0.3026	0.0425	0.0864	0.7125	0.7197	0.2611	0.3026	0.0426	0.0864	0.7124	0.7199
	Std	[0.0029]	[0.0025]	[0.0042]	[0.0019]	[0.0034]	[0.0032]	[0.0031]	[0.0011]	[0.0057]	[0.0019]	[0.0036]	[0.0034]
9-May	Mean	0.2444	0.3120	0.0537	0.0993	0.7150	0.7140	0.2443	0.3120	0.0538	0.0993	0.7151	0.7142
	Std	[0.0032]	[0.0028]	[0.0050]	[0.0023]	[0.0036]	[0.0036]	[0.0035]	[0.0013]	[0.0066]	[0.0024]	[0.0037]	[0.0038]
10-May	Mean	0.2649	0.3016	0.0215	0.1018	0.6928	0.6947	0.2649	0.3017	0.0216	0.1018	0.6929	0.6950

	Std	[0.0028]	[0.0026]	[0.0045]	[0.0022]	[0.0036]	[0.0036]	[0.0030]	[0.0012]	[0.0060]	[0.0022]	[0.0037]	[0.0037]
11-May	Mean	0.2723	0.3120	0.0152	0.1029	0.6838	0.6937	0.2722	0.3120	0.0151	0.1031	0.6841	0.6937
	Std	[0.0027]	[0.0026]	[0.0044]	[0.0022]	[0.0036]	[0.0034]	[0.0029]	[0.0012]	[0.0059]	[0.0022]	[0.0037]	[0.0035]
12-May	Mean	0.2584	0.3166	0.0388	0.1034	0.6916	0.7048	0.2584	0.3166	0.0387	0.1035	0.6917	0.7047
	Std	[0.0029]	[0.0028]	[0.0047]	[0.0023]	[0.0036]	[0.0034]	[0.0032]	[0.0013]	[0.0061]	[0.0023]	[0.0037]	[0.0035]
15-May	Mean	0.2893	0.3077	0.0291	0.0847	0.6657	0.6884	0.2893	0.3077	0.0291	0.0847	0.6660	0.6882
	Std	[0.0026]	[0.0027]	[0.0041]	[0.0020]	[0.0037]	[0.0035]	[0.0028]	[0.0012]	[0.0053]	[0.0019]	[0.0037]	[0.0036]
16-May	Mean	0.2692	0.3086	0.0325	0.0949	0.6897	0.6893	0.2691	0.3086	0.0327	0.0948	0.6899	0.6894
	Std	[0.0027]	[0.0027]	[0.0044]	[0.0022]	[0.0035]	[0.0035]	[0.0029]	[0.0012]	[0.0057]	[0.0022]	[0.0036]	[0.0036]
17-May	Mean	0.2785	0.3375	0.0023	0.1194	0.6772	0.6788	0.2784	0.3375	0.0026	0.1193	0.6773	0.6790
	Std	[0.0026]	[0.0026]	[0.0044]	[0.0023]	[0.0034]	[0.0033]	[0.0028]	[0.0013]	[0.0057]	[0.0023]	[0.0034]	[0.0034]
18-May	Mean	0.2839	0.3057	0.0457	0.0810	0.6970	0.7007	0.2859	0.3080	0.0634	0.0680	0.6904	0.7102
	Std	[0.0025]	[0.0023]	[0.0037]	[0.0016]	[0.0030]	[0.0030]	[0.0052]	[0.0016]	[0.0157]	[0.0093]	[0.0049]	[0.0048]
19-May	Mean	0.2779	0.3022	0.0391	0.0869	0.6878	0.7030	0.2780	0.3023	0.0389	0.0869	0.6877	0.7031
	Std	[0.0031]	[0.0029]	[0.0048]	[0.0023]	[0.0040]	[0.0038]	[0.0034]	[0.0013]	[0.0065]	[0.0023]	[0.0042]	[0.0039]
22-May	Mean	0.2783	0.2909	0.0308	0.0851	0.7086	0.7169	0.2783	0.2909	0.0309	0.0851	0.7087	0.7169
	Std	[0.0031]	[0.0027]	[0.0047]	[0.0023]	[0.0039]	[0.0037]	[0.0034]	[0.0011]	[0.0065]	[0.0023]	[0.0041]	[0.0039]
23-May	Mean	0.3097	0.2871	0.0163	0.0783	0.7040	0.7026	0.3096	0.2871	0.0164	0.0784	0.7037	0.7029
	Std	[0.0025]	[0.0022]	[0.0037]	[0.0016]	[0.0033]	[0.0034]	[0.0027]	[0.0009]	[0.0049]	[0.0016]	[0.0034]	[0.0034]
24-May	Mean	0.2995	0.2877	0.0003	0.0902	0.7073	0.6925	0.2995	0.2878	0.0000	0.0903	0.7073	0.6924
	Std	[0.0027]	[0.0023]	[0.0043]	[0.0020]	[0.0037]	[0.0039]	[0.0030]	[0.0010]	[0.0059]	[0.0020]	[0.0039]	[0.0041]
25-May	Mean	0.2783	0.3150	0.0267	0.1026	0.6991	0.7116	0.2783	0.3150	0.0268	0.1026	0.6992	0.7118
	Std	[0.0034]	[0.0030]	[0.0056]	[0.0030]	[0.0041]	[0.0038]	[0.0037]	[0.0014]	[0.0074]	[0.0029]	[0.0043]	[0.0040]
26-May	Mean	0.2840	0.3109	0.0161	0.1012	0.6936	0.6912	0.2840	0.3109	0.0162	0.1012	0.6936	0.6914
	Std	[0.0029]	[0.0027]	[0.0047]	[0.0022]	[0.0037]	[0.0038]	[0.0032]	[0.0012]	[0.0062]	[0.0022]	[0.0039]	[0.0039]
29-May	Mean	0.2783	0.3706	0.0279	0.1219	0.6524	0.6839	0.2783	0.3708	0.0276	0.1220	0.6526	0.6839
	Std	[0.0043]	[0.0042]	[0.0074]	[0.0038]	[0.0058]	[0.0050]	[0.0048]	[0.0025]	[0.0097]	[0.0039]	[0.0059]	[0.0051]
30-May	Mean	0.2883	0.3094	0.0395	0.0871	0.6899	0.6906	0.2883	0.3094	0.0395	0.0871	0.6900	0.6907
	Std	[0.0030]	[0.0028]	[0.0047]	[0.0022]	[0.0038]	[0.0038]	[0.0033]	[0.0012]	[0.0063]	[0.0022]	[0.0039]	[0.0040]
31-May	Mean	0.3055	0.3030	0.0319	0.0801	0.6902	0.6880	0.3056	0.3030	0.0319	0.0800	0.6903	0.6881
	Std	[0.0029]	[0.0026]	[0.0043]	[0.0020]	[0.0037]	[0.0037]	[0.0031]	[0.0012]	[0.0058]	[0.0020]	[0.0038]	[0.0039]
1-Jun	Mean	0.2841	0.3155	0.0597	0.0830	0.7038	0.7000	0.2841	0.3156	0.0597	0.0829	0.7039	0.7001
	Std	[0.0036]	[0.0033]	[0.0055]	[0.0029]	[0.0041]	[0.0042]	[0.0038]	[0.0014]	[0.0073]	[0.0028]	[0.0042]	[0.0044]
2-Jun	Mean	0.3428	0.3876	-0.0602	0.1151	0.6933	0.6910	0.3156	0.3328	0.0269	0.0850	0.6825	0.6797
	Std	[0.0034]	[0.0030]	[0.0051]	[0.0023]	[0.0049]	[0.0050]	[0.0028]	[0.0012]	[0.0051]	[0.0017]	[0.0033]	[0.0034]
5-Jun	Mean	0.2854	0.3014	0.0411	0.0809	0.7075	0.7157	0.2852	0.3014	0.0415	0.0809	0.7080	0.7155
	Std	[0.0031]	[0.0026]	[0.0044]	[0.0019]	[0.0037]	[0.0035]	[0.0033]	[0.0011]	[0.0058]	[0.0019]	[0.0038]	[0.0036]
6-Jun	Mean	0.2984	0.2866	0.0212	0.0770	0.6939	0.6861	0.2984	0.2867	0.0213	0.0770	0.6941	0.6862
	Std	[0.0031]	[0.0028]	[0.0048]	[0.0023]	[0.0042]	[0.0044]	[0.0034]	[0.0012]	[0.0068]	[0.0023]	[0.0044]	[0.0047]

7-Jun	Mean	0.2918	0.2764	0.0335	0.0662	0.6963	0.7154	0.2917	0.2764	0.0336	0.0662	0.6963	0.7157
	Std	[0.0028]	[0.0024]	[0.0039]	[0.0015]	[0.0038]	[0.0036]	[0.0030]	[0.0010]	[0.0055]	[0.0015]	[0.0040]	[0.0038]
8-Jun	Mean	0.2780	0.2809	0.0372	0.0744	0.6977	0.7013	0.2780	0.2809	0.0372	0.0744	0.6978	0.7014
	Std	[0.0028]	[0.0025]	[0.0042]	[0.0018]	[0.0038]	[0.0037]	[0.0031]	[0.0011]	[0.0057]	[0.0018]	[0.0039]	[0.0039]
9-Jun	Mean	0.2740	0.2848	0.0473	0.0710	0.7067	0.7022	0.2740	0.2848	0.0470	0.0711	0.7067	0.7022
	Std	[0.0029]	[0.0027]	[0.0044]	[0.0020]	[0.0037]	[0.0039]	[0.0032]	[0.0011]	[0.0060]	[0.0020]	[0.0040]	[0.0041]
12-Jun	Mean	0.2704	0.2900	0.0280	0.0819	0.6982	0.7003	0.2703	0.2901	0.0282	0.0818	0.6985	0.7002
	Std	[0.0025]	[0.0024]	[0.0038]	[0.0016]	[0.0034]	[0.0034]	[0.0027]	[0.0010]	[0.0051]	[0.0016]	[0.0035]	[0.0037]
13-Jun	Mean	0.2808	0.2692	0.0216	0.0722	0.6994	0.7052	0.2808	0.2692	0.0216	0.0722	0.6995	0.7052
	Std	[0.0024]	[0.0022]	[0.0036]	[0.0016]	[0.0036]	[0.0035]	[0.0026]	[0.0009]	[0.0050]	[0.0016]	[0.0037]	[0.0037]
14-Jun	Mean	0.2834	0.3213	0.0471	0.0792	0.7045	0.7086	0.2835	0.3215	0.0467	0.0792	0.7045	0.7086
	Std	[0.0030]	[0.0028]	[0.0043]	[0.0020]	[0.0037]	[0.0037]	[0.0032]	[0.0013]	[0.0055]	[0.0019]	[0.0037]	[0.0037]
15-Jun	Mean	0.2804	0.2945	-0.0012	0.0942	0.6768	0.6736	0.2805	0.2945	-0.0013	0.0942	0.6770	0.6735
	Std	[0.0018]	[0.0019]	[0.0030]	[0.0015]	[0.0027]	[0.0028]	[0.0020]	[0.0008]	[0.0039]	[0.0015]	[0.0028]	[0.0029]
16-Jun	Mean	0.2665	0.2867	0.0361	0.0794	0.6972	0.7111	0.2664	0.2867	0.0362	0.0794	0.6976	0.7109
	Std	[0.0025]	[0.0023]	[0.0038]	[0.0017]	[0.0034]	[0.0033]	[0.0027]	[0.0010]	[0.0051]	[0.0017]	[0.0035]	[0.0034]
19-Jun	Mean	0.5552	0.5191	0.0163	0.0829	0.5173	0.9789	0.5523	0.5189	0.0170	0.0837	0.5243	0.9788
	Std	[0.0985]	[0.0158]	[0.1181]	[0.0406]	[0.0398]	[0.0113]	[0.0201]	[0.0024]	[0.0265]	[0.0073]	[0.0199]	[0.0017]
20-Jun	Mean	0.2551	0.3324	0.0216	0.1089	0.6974	0.6866	0.2550	0.3325	0.0213	0.1092	0.6973	0.6867
	Std	[0.0029]	[0.0027]	[0.0047]	[0.0023]	[0.0036]	[0.0038]	[0.0031]	[0.0014]	[0.0061]	[0.0023]	[0.0037]	[0.0039]
21-Jun	Mean	0.2455	0.3182	0.0431	0.1031	0.7172	0.6920	0.2454	0.3182	0.0431	0.1031	0.7171	0.6922
	Std	[0.0034]	[0.0032]	[0.0055]	[0.0027]	[0.0039]	[0.0043]	[0.0037]	[0.0015]	[0.0070]	[0.0027]	[0.0040]	[0.0044]
22-Jun	Mean	0.2467	0.3794	-0.0091	0.1424	0.6907	0.6939	0.2465	0.3797	-0.0094	0.1424	0.6906	0.6941
	Std	[0.0037]	[0.0032]	[0.0061]	[0.0032]	[0.0050]	[0.0048]	[0.0042]	[0.0025]	[0.0084]	[0.0034]	[0.0051]	[0.0049]
23-Jun	Mean	0.8224	0.7571	-0.0164	0.2003	0.5713	0.9278	0.8216	0.7572	-0.0166	0.2008	0.5712	0.9277
	Std	[0.0072]	[0.0022]	[0.0095]	[0.0037]	[0.0050]	[0.0010]	[0.0068]	[0.0017]	[0.0095]	[0.0037]	[0.0048]	[0.0009]
26-Jun	Mean	0.2759	0.4503	-0.1332	0.1794	0.7824	0.6354	0.2600	0.3801	-0.0108	0.1281	0.6979	0.6735
	Std	[0.0108]	[0.0034]	[0.0055]	[0.0047]	[0.0222]	[0.0110]	[0.0032]	[0.0019]	[0.0052]	[0.0024]	[0.0042]	[0.0045]
27-Jun	Mean	0.2684	0.3322	0.0086	0.1072	0.6744	0.6796	0.2684	0.3323	0.0085	0.1073	0.6745	0.6796
	Std	[0.0029]	[0.0029]	[0.0046]	[0.0023]	[0.0040]	[0.0040]	[0.0032]	[0.0015]	[0.0061]	[0.0023]	[0.0041]	[0.0040]
28-Jun	Mean	0.2571	0.3190	0.0003	0.1126	0.6886	0.6757	0.2570	0.3191	0.0005	0.1126	0.6889	0.6759
	Std	[0.0028]	[0.0028]	[0.0047]	[0.0023]	[0.0038]	[0.0040]	[0.0031]	[0.0014]	[0.0060]	[0.0023]	[0.0039]	[0.0041]
29-Jun	Mean	0.2597	0.3010	0.0179	0.0979	0.7011	0.6973	0.2598	0.3011	0.0179	0.0978	0.7013	0.6974
	Std	[0.0028]	[0.0027]	[0.0043]	[0.0021]	[0.0036]	[0.0036]	[0.0030]	[0.0012]	[0.0057]	[0.0021]	[0.0036]	[0.0037]
Average	Mean	0.2945	0.3298	0.0208	0.0986	0.6897	0.7079	0.2970	0.3350	0.0264	0.0982	0.6910	0.7086

Table 7. The extended GH Model (GH) : MLE on 19 and 23 June 2016

$$p_i = m_i + cq_i, m_i = m_{i-1} + \lambda_i (q_i - E[q_i | \Omega_{i-1}]) + u_i, u_i \sim N(0, \sigma_u^2), q_i \in \{-1, 1\}$$

where $\Pr[q_i = 1 | q_{i-1} = 1] = P, \Pr[q_i = -1 | q_{i-1} = -1] = Q$ and $\lambda_i = \lambda_0 + \lambda_1 \sqrt{V_i}$

This table provides the MLE estimates of the above model for every 10,000 trade using the gold futures contract traded on the CME Globex electronic trading platform on May 19, 2016 and June 23, 2016. (See the caption of Table 2 for further details on the dating convention used in the paper.) σ_u is the standard deviation of the (log) efficient price changes: c is the order processing component of the (log) half spread. P and Q are transition probabilities. λ_0 and λ_1 are the fixed and variable permanent price impact costs, respectively, due to adverse selection. In this table, 10,000 fold of c , λ_0 , λ_1 , and σ_u estimates are reported.

Panel A.		GH							
		Intervals	19.Jun	$c \times 10,000$	$\sigma_u \times 10,000$	$\lambda_0 \times 10,000$	$\lambda_1 \times 10,000$	P	Q
1	to 10,000			6.4691 [0.2488]	1.1455 [0.0092]	0.4026 [0.2663]	0.2973 [0.0296]	0.7779 [0.0285]	0.9952 [0.0007]
2	to 20,000			0.2369 [0.0070]	0.3296 [0.0067]	0.0224 [0.0112]	0.1079 [0.0045]	0.6998 [0.0093]	0.6812 [0.0103]
3	to 30,000			0.2618 [0.0067]	0.3253 [0.0067]	-0.0045 [0.0107]	0.1143 [0.0045]	0.6932 [0.0084]	0.6696 [0.0093]
4	to 40,000			3.8289 [0.3346]	0.4982 [0.0047]	0.1617 [0.3525]	0.0132 [0.0140]	0.9756 [0.0055]	0.9978 [0.0005]
5	over 40,000			0.2338 [0.0056]	0.3163 [0.0051]	0.0279 [0.0088]	0.1034 [0.0037]	0.7129 [0.0070]	0.7193 [0.0066]
	Average			2.2061 [0.0726]	0.5230 [0.0067]	0.1220 [0.0910]	0.1272 [0.0072]	0.7719 [0.0083]	0.8126 [0.0011]

Panel B.		GH							
		Intervals	23.Jun	$c \times 10,000$	$\sigma_u \times 10,000$	$\lambda_0 \times 10,000$	$\lambda_1 \times 10,000$	P	Q
1	to 10,000			0.5888 [0.0379]	0.8663 [0.0154]	0.0013 [0.0413]	0.2801 [0.0159]	0.6134 [0.0293]	0.8806 [0.0113]
2	to 20,000			0.4937 [0.0178]	0.7023 [0.0096]	-0.1802 [0.0266]	0.3249 [0.0132]	0.6875 [0.0224]	0.7321 [0.0199]
3	to 30,000			0.5979 [0.0160]	0.6508 [0.0085]	-0.0602 [0.0237]	0.2135 [0.0118]	0.7514 [0.0121]	0.6862 [0.0158]
4	to 40,000			0.7480 [0.0229]	0.8385 [0.0118]	-0.2228 [0.0331]	0.3381 [0.0152]	0.8047 [0.0117]	0.6680 [0.0198]
5	to 50,000			0.6967 [0.0161]	0.7770 [0.0099]	-0.1401 [0.0247]	0.3168 [0.0107]	0.5469 [0.0126]	0.7715 [0.0072]
6	to 60,000			1.9791 [0.0767]	1.4917 [0.0144]	-0.3999 [0.0944]	0.5310 [0.0365]	0.4938 [0.0215]	0.9656 [0.0026]
7	to 70,000			1.8634 [0.0993]	1.6498 [0.0175]	-0.6026 [0.1156]	0.7196 [0.0381]	0.5066 [0.0268]	0.9635 [0.0035]
8	to 80,000			0.9524	0.9531	-0.2908	0.4380	0.5595	0.8842

		[0.0301]	[0.0120]	[0.0418]	[0.0199]	[0.0173]	[0.0061]
9	to 90,000	0.7291 [0.0530]	0.8546 [0.0115]	-0.3889 [0.0559]	0.4027 [0.0250]	0.3652 [0.0323]	0.9482 [0.0077]
10	to 100,000	0.6063 [0.0479]	0.8177 [0.0141]	-0.2904 [0.0448]	0.3642 [0.0216]	0.9135 [0.0122]	0.5138 [0.0281]
11	to 110,000	0.4745 [0.0192]	0.6399 [0.0100]	-0.0942 [0.0242]	0.2284 [0.0110]	0.6774 [0.0261]	0.7772 [0.0203]
12	to 120,000	0.4426 [0.0207]	0.6456 [0.0108]	-0.1777 [0.0264]	0.2620 [0.0133]	0.8207 [0.0133]	0.5577 [0.0259]
13	to 130,000	0.4085 [0.0757]	0.5672 [0.0111]	-0.2453 [0.0387]	0.2824 [0.0199]	0.9430 [0.0172]	0.5707 [0.0281]
14	to 140,000	0.1929 [0.0117]	0.4566 [0.0071]	-0.1674 [0.0150]	0.2202 [0.0070]	0.6016 [0.0173]	0.6904 [0.0168]
15	to 150,000	0.2419 [0.0082]	0.3689 [0.0069]	-0.0944 [0.0131]	0.1850 [0.0066]	0.6870 [0.0126]	0.6956 [0.0114]
16	to 160,000	0.0879 [0.0107]	0.4589 [0.0055]	-0.2227 [0.0214]	0.2584 [0.0085]	0.4040 [0.0489]	0.2585 [0.0313]
17	over 160,000	0.8761 [0.0719]	0.5628 [0.0052]	-0.0550 [0.0754]	0.1364 [0.0192]	0.9928 [0.0013]	0.5789 [0.0604]
	Average	0.7047 [0.0318]	0.7825 [0.0106]	-0.2136 [0.0370]	0.3236 [0.0156]	0.6688 [0.0082]	0.7143 [0.0085]

Table 8. Classified Trades: Correlations

This table provides daily correlation estimates of the classified trades using the Tick rule, the Roll model, and the extended GH model for the gold futures contract traded on the CME Globex electronic trading platform from May 1, 2016 to June 30, 2016. (See the caption of Table 2 for further details on the dating convention used in the paper). The daily correlations of classified trades between the Tick rule and the Roll model (the extended GH model) is labelled as Roll (GH) respectively.

Date	Roll	GH
1-May	0.9999	0.9984
2-May	1.0000	0.9991
3-May	0.9980	0.9988
4-May	0.9994	0.9995
5-May	1.0000	0.9975
8-May	0.9995	0.9998
9-May	1.0000	0.9996
10-May	1.0000	0.9998
11-May	0.9999	0.9995
12-May	1.0000	0.9994
15-May	1.0000	0.9996
16-May	1.0000	0.9999
17-May	0.9996	0.9991
18-May	1.0000	0.9999
19-May	1.0000	0.9999
22-May	0.9999	0.9998
23-May	1.0000	1.0000
24-May	1.0000	0.9990
25-May	0.9999	1.0000
26-May	0.9995	0.9997
29-May	0.9998	0.9949
30-May	1.0000	1.0000
31-May	1.0000	1.0000
1-Jun	1.0000	0.9999
2-Jun	0.9998	0.9939
5-Jun	1.0000	0.9998
6-Jun	1.0000	1.0000
7-Jun	1.0000	1.0000
8-Jun	1.0000	0.9999
9-Jun	1.0000	1.0000
12-Jun	0.9995	0.9997
13-Jun	1.0000	1.0000
14-Jun	0.9995	0.9996
15-Jun	1.0000	0.9997
16-Jun	1.0000	0.9998
19-Jun	0.9887	0.6063
20-Jun	0.9995	0.9977
21-Jun	0.9991	0.9960
22-Jun	0.9989	0.9839
23-Jun	0.9988	0.4455
26-Jun	0.9991	0.8260
27-Jun	0.9993	0.9976
28-Jun	1.0000	0.9979
29-Jun	0.9997	0.9996

Table 9. The Bid-Ask Spread (ticks) and Relative Decomposition

$$p_t = m_t + cq_t, m_t = m_{t-1} + \lambda_i (q_t - E[q_t | \Omega_{t-1}]) + u_t, u_t \sim N(0, \sigma_u^2), q_t \in \{-1, 1\}$$

$$\text{where } \Pr[q_t = 1 | q_{t-1} = 1] = P, \Pr[q_t = -1 | q_{t-1} = -1] = Q \text{ and } \lambda_i = \lambda_0 + \lambda_1 \sqrt{V_t}$$

This table gives daily bid-ask spread in ticks and estimates of liquidity components of the above model with data from gold futures contracts traded on the CME Globex electronic trading platform from May 1, 2016 to June 30, 2016. (See the caption of Table 2 for further details on the dating convention used in the paper) In this model, σ_u is the standard deviation of the log efficient price changes: c is the order processing component of the (log) half spread. P and Q are transition probabilities. λ_0 and λ_1 are the fixed and variable permanent price impact costs, respectively. In particular, this table first reports $S_{GH,cs}$ which is the spread in ticks computed as $S_{GH,cs} = sp_{GH,cs} \times \bar{P}$ where $sp_{GH,cs}$ is the log spread estimates implied by the model with the daily average volume per trade (\bar{V}_t) (i.e., computed as $sp_{GH,cs} = 2 \times (c + \lambda_0 + \lambda_1 \sqrt{\bar{V}_t})$), and \bar{P} is the average daily tick price. For example, the $S_{GH,cs}$ on 1, May is 1.1970 (i.e., $2 \times (0.4615 \times 10^{-4}) \times (1,296.9/0.1)$) where 1,296.9 is the mean of the daily prices and 0.1 is the tick size on 1, May. In the last two columns, the estimates of informational and non-informational components of the bid-ask spread ($S_{GH,cs}$) are computed using the results in Table 6 as follows.

$$\text{Proportion of spread arising from order processing cost component : } \text{TC} = c / (c + (\lambda_0 + \lambda_1 \sqrt{\bar{V}_t}))$$

$$\text{Proportion of spread arising from the information asymmetry component: } \text{IC} = (\lambda_0 + \lambda_1 \sqrt{\bar{V}_t}) / (c + (\lambda_0 + \lambda_1 \sqrt{\bar{V}_t}))$$

Date	AVG. daily price	\bar{V}	$sp_{GH,cs}$	$S_{GH,cs}$	TC	IC
1-May	1296.9	2.87	0.9229	1.1970	0.5254	0.4746
2-May	1294.3	2.85	0.9312	1.2053	0.5749	0.4251
3-May	1283.4	2.90	0.9457	1.2138	0.5751	0.4249
4-May	1280.6	2.84	0.9288	1.1894	0.5593	0.4407
5-May	1289.1	2.88	0.9471	1.2209	0.5719	0.4281
8-May	1274.3	3.03	0.9081	1.1572	0.5751	0.4249
9-May	1265.0	2.80	0.9288	1.1750	0.5262	0.4738
10-May	1275.5	2.93	0.9217	1.1755	0.5749	0.4251
11-May	1273.2	2.93	0.9274	1.1808	0.5872	0.4128
12-May	1270.9	2.82	0.9419	1.1971	0.5486	0.4514
15-May	1281.0	3.06	0.9330	1.1952	0.6201	0.3799
16-May	1277.5	2.96	0.9294	1.1873	0.5792	0.4208
17-May	1271.3	2.93	0.9656	1.2275	0.5768	0.4232
18-May	1252.7	3.32	0.9545	1.1956	0.5948	0.4052
19-May	1255.3	2.95	0.9327	1.1708	0.5960	0.4040
22-May	1249.8	2.82	0.9038	1.1296	0.6159	0.3841

23-May	1237.6	3.34	0.9385	1.1615	0.6601	0.3399
24-May	1223.2	3.16	0.9197	1.1250	0.6512	0.3488
25-May	1226.5	2.71	0.9481	1.1627	0.5871	0.4129
26-May	1216.6	3.18	0.9614	1.1320	0.5909	0.4091
29-May	1207.7	2.82	1.0215	1.2336	0.5448	0.4552
30-May	1215.3	2.96	0.9551	1.1608	0.6037	0.3963
31-May	1216.4	2.99	0.9518	1.1577	0.6420	0.3580
1-Jun	1215.7	2.70	0.9601	1.1672	0.5919	0.4081
2-Jun	1234.1	3.30	0.9830	1.2132	0.6974	0.3026
5-Jun	1246.2	3.05	0.9357	1.1660	0.6101	0.3899
6-Jun	1243.9	3.02	0.9068	1.1279	0.6582	0.3418
7-Jun	1258.8	3.39	0.8941	1.1254	0.6527	0.3473
8-Jun	1267.0	3.09	0.8917	1.1298	0.6234	0.3766
9-Jun	1273.8	3.13	0.8936	1.1383	0.6131	0.3869
12-Jun	1284.0	3.19	0.8893	1.1419	0.6081	0.3919
13-Jun	1286.5	3.14	0.8607	1.1073	0.6525	0.3475
14-Jun	1289.6	3.01	0.9358	1.2068	0.6057	0.3943
15-Jun	1305.1	3.17	0.8965	1.1699	0.6256	0.3744
16-Jun	1290.6	3.07	0.8832	1.1398	0.6034	0.3966
19-Jun	1287.6	3.18	4.8659	6.2654	0.9068	0.0932
20-Jun	1278.5	3.03	0.9329	1.1927	0.5469	0.4531
21-Jun	1269.4	2.84	0.9245	1.1735	0.5312	0.4688
22-Jun	1266.0	2.69	0.9600	1.2154	0.5140	0.4860
23-Jun	1315.0	2.88	2.0815	3.2990	0.6771	0.3229
26-Jun	1330.2	2.83	0.8891	1.1827	0.6206	0.3794
27-Jun	1317.7	2.96	0.9061	1.1940	0.5925	0.4075
28-Jun	1323.8	3.01	0.9052	1.1982	0.5681	0.4319
29-Jun	1320.8	3.03	0.8958	1.1359	0.5799	0.4201

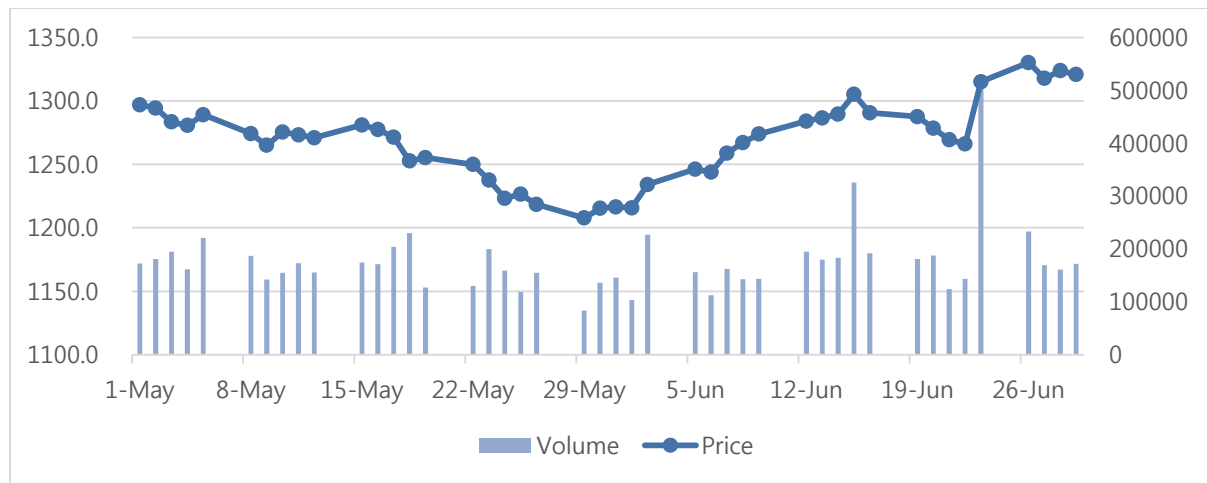


Figure 1: Daily series of average prices (Price) and trading volumes (Volume)

This figure presents the daily series of average prices (Price) and trading volumes (Volume) of the gold futures contract from May 1, 2016 to June 30, 2016. (See the caption of Table 2 for further details on the dating convention used in the paper)

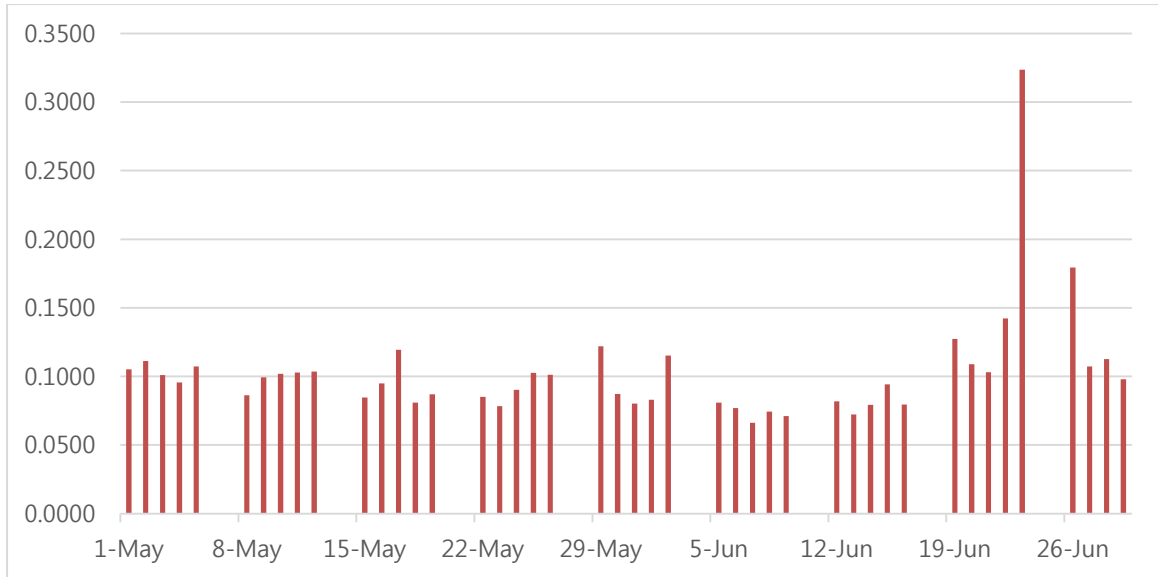


Figure 2: Daily estimates of the permanent price impact

$$p_t = m_t + cq_t, m_t = m_{t-1} + \lambda_t (q_t - E[q_t | \Omega_{t-1}]) + u_t, u_t \sim N(0, \sigma_u^2), q_t \in \{-1, 1\}$$

$$\text{where } \Pr[q_t = 1 | q_{t-1} = 1] = P, \Pr[q_t = -1 | q_{t-1} = -1] = Q \text{ and } \lambda_t = \lambda_0 + \lambda_1 \sqrt{V_t}$$

This figure provides daily λ_t estimates from the above model using data on gold futures contracts trading on the CME Globex electronic trading platform from May 1, 2016 to June 30, 2016. (See the caption of Table 2 for further details on the dating convention used in the paper.) In this model, σ_u is the standard deviation of the log efficient price changes: c is the order processing component of the (log) half spread. P and Q are transition probabilities. λ_0 and λ_1 are the fixed and variable permanent price impact costs, respectively.

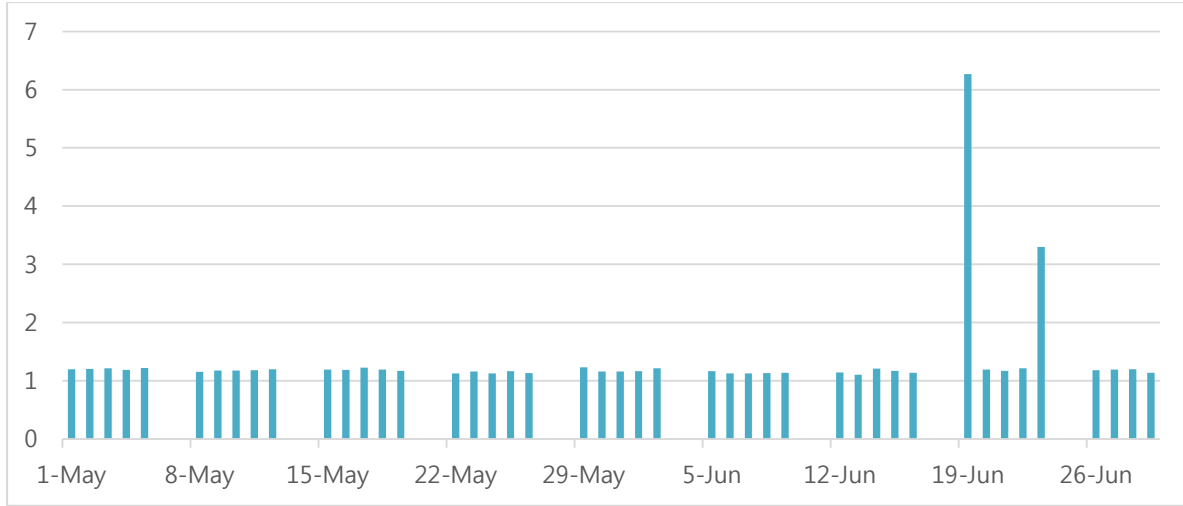


Figure 3: The Bid-Ask Spread in ticks

$$p_t = m_t + cq_t, m_t = m_{t-1} + \lambda_t (q_t - E[q_t | \Omega_{t-1}]) + u_t, u_t \sim N(0, \sigma_u^2), q_t \in \{-1, 1\}$$

$$\text{where } \Pr[q_t = 1 | q_{t-1} = 1] = P, \Pr[q_t = -1 | q_{t-1} = -1] = Q \text{ and } \lambda_t = \lambda_0 + \lambda_1 \sqrt{V_t}$$

This figure presents daily bid-ask spread in ticks of the above model using data from gold futures contracts trading on the CME Globex electronic trading platform from May 1, 2016 to June 30, 2016. (See the caption of Table 2 for further details on the dating convention used in the paper.) In this model, σ_u is the standard deviation of the log efficient price changes: c is the order processing component of the (log) half spread. P and Q are transition probabilities. λ_0 and λ_1 are the fixed and variable permanent price impact costs, respectively. In particular, this table first reports $S_{GH,cs}$ which is the spread in ticks computed as $S_{GH,cs} = sp_{GH,cs} \times \bar{P}$ where $sp_{GH,cs}$ is the log spread estimates implied by the model with the daily average volume (\bar{V}_t) (i.e., computed as $sp_{GH,cs} = 2 \times (c + \lambda_0 + \lambda_1 \sqrt{\bar{V}_t})$), and \bar{P} is the average daily tick price. For example, the $S_{GH,cs}$ on 1, May is 1.1970 (i.e., $2 \times (0.4615 \times 10^{-4}) \times (1,296.9/0.1)$) where 1,296.9 is the mean of the daily prices and 0.1 is the tick size on 1, May.

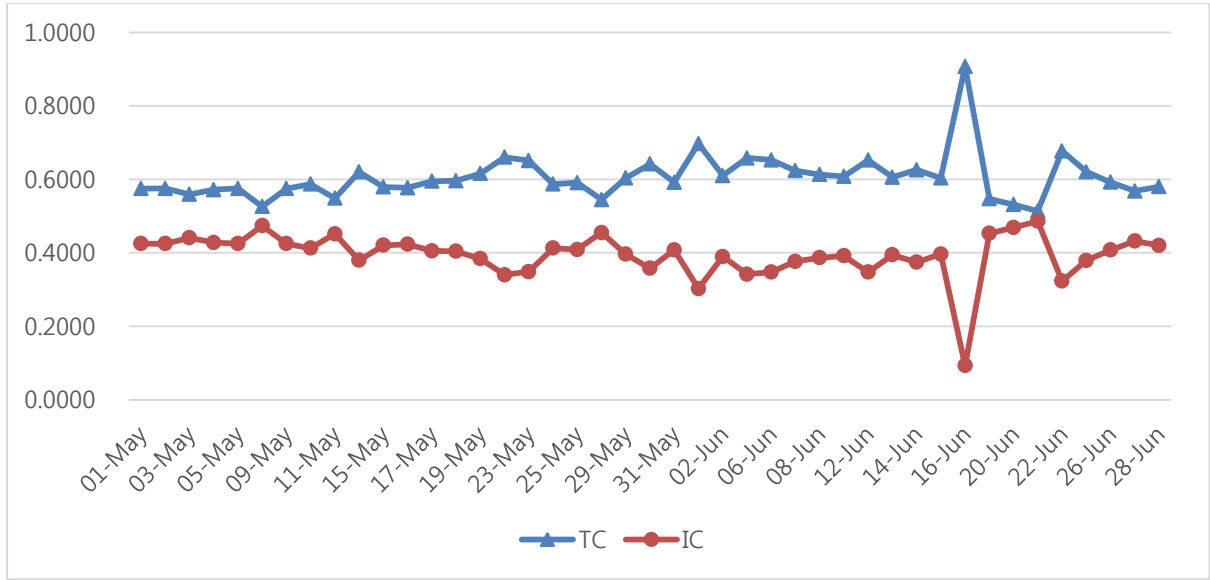


Figure 4: Daily estimates of informational (IC) and non-informational (TC) components

$$p_t = m_t + cq_t, m_t = m_{t-1} + \lambda_t (q_t - E[q_t | \Omega_{t-1}]) + u_t, u_t \sim N(0, \sigma_u^2), q_t \in \{-1, 1\}$$

$$\text{where } \Pr[q_t = 1 | q_{t-1} = 1] = P, \Pr[q_t = -1 | q_{t-1} = -1] = Q \text{ and } \lambda_t = \lambda_0 + \lambda_1 \sqrt{V_t}$$

This figure presents daily estimates of liquidity components of the above model using gold futures data from contracts trading on the CME Globex electronic trading platform from May 1, 2016 to June 30, 2016 (See the caption of Table 2 for further details on the dating convention used in the paper.) In this model, σ_u is the standard deviation of the log efficient price changes: c is the order processing component of the (log) half spread. P and Q are transition probabilities. λ_0 and λ_1 are the fixed and variable permanent price impact costs, respectively. In particular, the estimates of informational and non-informational components of the bid-ask spread ($S_{GH,cs}$) are computed using the results in Table 6 as follows.

$$\text{Proportion of spread arising from order processing cost component: } \text{TC} = c / (c + (\lambda_0 + \lambda_1 \sqrt{V_t}))$$

$$\text{Proportion of spread arising from the information asymmetry component: } \text{IC} = (\lambda_0 + \lambda_1 \sqrt{V_t}) / (c + (\lambda_0 + \lambda_1 \sqrt{V_t}))$$

APPENDICES

Table A1. Convergence diagnostics for the Bayesian estimation

This table provides two convergence diagnostics for the Bayesian estimation of the three models: Roll, the extended Roll, and the extended GH. In particular, we compute and report the effective sample size based on the inefficiency factors and the p-value of Geweke(1992)'s convergence diagnostics test for the model parameters.

- 1) **Geweke(1992)'s convergence diagnostic:** if Geweke's p-value is less than 0.05, we interpret the burn-in period is too small and we can't guarantee the convergence of the chain. In general, as Geweke's p-value is close to 1, we have more efficient samples.
- 2) **Inefficiency factor and effective sample size:** the effective sample size should be larger than 1000 for all parameters to guarantee sufficient number of the MCMC draws.

Refer to Appendix B for more details on the inefficiency factors and the Geweke(1992)'s diagnostic tests.

		Roll (Bayesian)				MS(Bayeisan)				GH(Bayeisan)			
Date	Parameters	c	σ_u	c	σ_u	P	Q	c	σ_u	λ_0	λ_1	P	Q
1-May	Geweke P	0.9274	0.7340	0.7009	0.4356	0.5952	0.6594	0.5929	0.7866	0.5419	0.8123	0.6971	0.1978
	Effective size	8413	8998	11709	9239	1761	1809	9405	6301	5210	9793	3988	3772
2-May	Geweke P	0.7120	0.8444	0.7632	0.7944	0.9771	0.6380	0.9897	0.9338	0.9901	0.9178	0.3291	0.9217
	Effective size	6693	6940	13726	13494	2203	2292	10202	8163	5358	11294	4305	4866
3-May	Geweke P	0.9605	0.9132	0.8327	0.7237	0.9632	0.9860	0.6982	0.9823	0.8535	0.9734	0.7017	0.8055
	Effective size	8322	8432	13122	11211	1586	1615	10009	7062	5094	7955	3083	3163
4-May	Geweke P	0.7671	0.7688	0.9416	0.7742	0.8531	0.8939	0.5546	0.4763	0.7750	0.9529	0.7296	0.1347
	Effective size	7091	7830	14005	13976	2098	2068	8863	7376	4871	10748	3995	3889
5-May	Geweke P	0.9031	0.8974	0.5375	0.6463	0.1675	0.3989	0.5032	0.0945	0.3977	0.8397	0.7748	0.7234
	Effective size	8556	9566	12791	8561	1410	1440	10337	6100	5620	10743	3702	3730
8-May	Geweke P	0.7246	0.9435	0.9898	0.8651	0.7313	0.8059	0.3239	0.6552	0.6819	0.8941	0.8464	0.8006
	Effective size	7552	8164	15635	16948	2039	2308	6978	9673	4153	8696	3292	4265
9-May	Geweke P	0.9923	0.9756	0.6797	0.5197	0.6723	0.7198	0.9466	0.6883	0.7881	0.9219	0.8683	0.8723
	Effective size	7312	8065	13524	16028	2228	2239	9148	9055	4902	10650	4548	4300
10-May	Geweke P	0.8597	0.8468	0.9085	0.9910	0.8637	0.8849	0.9912	0.9483	0.8477	0.9829	0.5173	0.5464
	Effective size	4355	4450	16384	22530	2478	2411	9797	10977	5277	11881	4414	4630
11-May	Geweke P	0.7258	0.7233	0.9749	0.9444	0.7256	0.7679	0.9873	0.8992	0.6461	0.9855	0.8663	0.7997
	Effective size	6011	6048	15662	16480	2442	2521	9102	9629	5154	9822	4496	4650
12-May	Geweke P	0.4671	0.1306	0.8781	0.8194	0.5045	0.4020	0.8810	0.8251	0.4436	0.6628	0.7698	0.8778

	Effective size	5998	6269	15485	14156	2336	2521	10673	8176	5254	10002	4387	5525
15-May	Geweke P	0.9804	0.9910	0.7367	0.9856	0.2007	0.8215	0.5584	0.6684	0.7590	0.8321	0.9885	0.9578
	Effective size	1110	1104	19063	22743	2440	2581	9392	9749	5663	14534	4491	4378
16-May	Geweke P	0.9861	0.9982	0.9812	0.8226	0.8437	0.9154	0.9140	0.6349	0.9917	0.8659	0.9325	0.9850
	Effective size	4731	4964	16268	21081	2479	2479	10010	10550	5697	11989	4254	4262
17-May	Geweke P	0.9408	0.9837	0.9529	0.9817	0.8258	0.7747	0.9903	0.7454	0.8285	0.6952	0.9203	0.9801
	Effective size	6925	7316	13956	11694	1777	1823	9781	7233	5551	9936	3902	4169
18-May	Geweke P	0.9808	0.9915	0.7779	0.8919	0.5869	0.5827	0.9980	0.9564	0.9744	0.9993	0.9060	0.7648
	Effective size	2755	2765	18418	23314	2695	2865	22352	25950	47455	170478	10429	12956
19-May	Geweke P	0.8704	0.8706	0.9976	0.7876	0.9471	0.9925	0.8460	0.9024	0.7672	0.7379	0.8028	0.6164
	Effective size	1915	1920	17516	25642	2995	3043	9078	11419	5420	14514	4634	5869
22-May	Geweke P	0.8781	0.8970	0.9675	0.9082	0.9316	0.9432	0.7572	0.9166	0.9321	0.2853	0.6214	0.5764
	Effective size	2498	2554	16569	33538	2555	2635	6881	12558	4287	12419	3653	4609
23-May	Geweke P	0.7080	0.8577	0.8650	0.8628	0.4451	0.0017	0.8091	0.9661	0.9791	0.9982	0.9101	0.9036
	Effective size	10768	10680	18213	39618	1970	2016	7423	15025	4428	11320	3793	3681
24-May	Geweke P	0.4406	0.6900	0.7203	0.8073	0.9700	0.8814	0.6428	0.7684	0.7129	0.7195	0.8326	0.4196
	Effective size	9734	8897	17721	40108	2246	2086	8064	22279	4768	9563	4227	4033
25-May	Geweke P	0.8894	0.8665	0.9421	0.8548	0.7626	0.7971	0.9654	0.9888	0.8617	0.6404	0.9288	0.9292
	Effective size	6131	6708	18609	20088	2407	2504	8048	9792	4614	8849	3835	4483
26-May	Geweke P	0.4039	0.8067	0.9523	0.9749	0.9754	0.9128	0.2232	0.6810	0.4580	0.6544	0.3993	0.4403
	Effective size	5997	6121	17895	21393	2468	2548	10901	13522	5272	8721	4332	4447
29-May	Geweke P	0.8549	0.8375	0.9162	0.9685	0.7571	0.1063	0.7973	0.5983	0.6381	0.8937	0.5263	0.0568
	Effective size	7427	7657	11083	9611	2219	2498	10980	6422	6110	11504	3862	5104
30-May	Geweke P	0.8045	0.8141	0.7647	0.9484	0.7140	0.6880	0.6616	0.9484	0.8442	0.9858	0.4684	0.9291
	Effective size	3001	2921	19121	28204	3115	3053	8867	11798	5117	13621	4875	4487
31-May	Geweke P	0.8063	0.7697	0.5694	0.9738	0.6201	0.7709	0.6797	0.7483	0.1615	0.4906	0.8193	0.8537
	Effective size	11536	10198	22675	40217	3217	3210	8190	12667	5347	14808	4416	4129
1-Jun	Geweke P	0.9828	0.9945	0.9642	0.6798	0.9261	0.9397	0.5620	0.6319	0.2861	0.7874	0.4802	0.9943
	Effective size	1921	1920	16855	23509	3054	2898	8539	10738	5241	11107	4903	4214
2-Jun	Geweke P	0.9627	0.8922	0.8057	0.6785	0.8385	0.7904	0.4829	0.6432	0.5624	0.1216	0.7074	0.9768
	Effective size	9166	10011	2100	3996	1593	2303	8562	8948	5794	16780	3924	3970
5-Jun	Geweke P	0.7646	0.7154	0.9174	0.8756	0.9172	0.8797	0.8476	0.7030	0.2764	0.6942	0.5404	0.8952
	Effective size	4603	4810	17471	25441	2046	2098	7583	10716	4823	12453	3758	4054
6-Jun	Geweke P	0.9076	0.8397	0.8185	0.9313	0.9465	0.8586	0.9260	0.5150	0.7924	0.7595	0.9570	0.9982
	Effective size	14111	12035	20441	46255	3599	3606	7152	14816	4388	11504	4585	3779
7-Jun	Geweke P	0.9111	0.9243	0.3407	0.9785	0.6226	0.7852	0.8492	0.7661	0.7781	0.6150	0.3032	0.6276
	Effective size	12290	11849	20534	44770	2900	2987	6984	16289	4173	13000	4067	4286
8-Jun	Geweke P	0.9028	0.7456	0.9511	0.9431	0.6865	0.6674	0.6449	0.6903	0.3703	0.7814	0.9207	0.9178
	Effective size	9966	9624	20373	41532	3583	3449	8571	15989	5009	12590	4736	4527
9-Jun	Geweke P	0.6104	0.4483	0.9445	0.9229	0.9531	0.9779	0.6278	0.8647	0.1998	0.8142	0.6720	0.1087
	Effective size	6233	6095	17409	34046	3001	2882	8419	13675	4854	12705	4078	3924

12-Jun	Geweke P	0.8979	0.8997	0.8840	0.7422	0.5844	0.8830	0.8565	0.3687	0.5347	0.6629	0.8213	0.5067
	Effective size	4340	4408	16462	24304	2508	2432	8792	12149	4823	11415	3772	3205
13-Jun	Geweke P	0.2990	0.7920	0.9485	0.9339	0.9445	0.8870	0.9135	0.9903	0.9949	0.9700	0.7857	0.8169
	Effective size	10497	9993	18318	44846	2824	2754	7583	19914	4421	11163	3725	3829
14-Jun	Geweke P	0.9301	0.9365	0.7596	0.8193	0.7304	0.7161	0.8014	0.9051	0.8559	0.9507	0.9008	0.7635
	Effective size	7551	7924	14613	11401	1299	1278	7698	7484	5386	11745	2985	2777
15-Jun	Geweke P	0.9551	0.9655	0.9315	0.9434	0.8175	0.7730	0.9280	0.8710	0.9975	0.9427	0.6644	0.6701
	Effective size	3767	3785	19552	24541	2649	2604	6351	12261	3669	6334	3840	3211
16-Jun	Geweke P	0.9779	0.9994	0.9391	0.9648	0.5655	0.5579	0.7463	0.7460	0.7892	0.7972	0.5594	0.9741
	Effective size	3350	3386	17458	28623	2255	2355	8194	12251	4583	11865	4021	4214
19-Jun	Geweke P	0.9612	0.9813	0.3395	0.3643	0.1126	0.3096	0.3752	0.4261	0.4189	0.3922	0.3181	0.3925
	Effective size	10292	12942	1795	5090	1443	2416	1761	1855	1800	1754	1336	1130
20-Jun	Geweke P	0.9796	0.9958	0.9473	0.5442	0.9371	0.8569	0.8620	0.9588	0.9405	0.9189	0.9376	0.9126
	Effective size	8563	9767	10851	9542	1813	1761	10706	7066	5464	8889	3483	3194
21-Jun	Geweke P	0.6503	0.8400	0.9390	0.7055	0.7626	0.8244	0.8835	0.7967	0.8501	0.4754	0.7167	0.9325
	Effective size	8429	9114	12092	11998	2339	2167	10139	8849	5454	10399	4308	3487
22-Jun	Geweke P	0.7910	0.9317	0.8806	0.9841	0.8713	0.8793	0.9420	0.8065	0.8815	0.9087	0.7090	0.7914
	Effective size	8430	9672	8324	5570	1102	1119	2765	2468	1689	2426	2231	2358
23-Jun	Geweke P	0.9840	0.9498	0.9698	0.2067	0.0281	0.3924	0.5930	0.8584	0.8570	0.8807	0.3825	0.7881
	Effective size	12473	16675	3445	3441	1404	3537	2175	3563	2160	2260	1533	2951
26-Jun	Geweke P	0.9672	0.9994	0.9156	0.7016	0.9716	0.3641	0.8711	0.7982	0.9228	0.7864	0.4213	0.3246
	Effective size	10103	12038	2206	3219	2184	1168	1272	2429	1068	1255	2002	1894
27-Jun	Geweke P	0.7884	0.7695	0.9528	0.9358	0.9717	0.9076	0.7976	0.5119	0.5352	0.7927	0.5152	0.3013
	Effective size	8078	8351	12859	8734	1761	1914	9493	6378	5683	11834	3190	3189
28-Jun	Geweke P	0.7134	0.9336	0.9197	0.7476	0.3981	0.3297	0.7854	0.9133	0.9032	0.9169	0.8185	0.8430
	Effective size	7551	7955	13293	11938	1875	1817	8604	6969	4565	8044	4115	3649
29-Jun	Geweke P	0.7966	0.6836	0.9112	0.8719	0.8441	0.9496	0.8172	0.8332	0.8920	0.8856	0.7177	0.7762
	Effective size	7797	8246	14997	15705	2072	2067	9272	9592	5147	9459	4436	4205

Table A.2 The difference of estimates from Bayes and MLE

This table presents average and maximum absolute differences between parameter estimates based on MLE and Bayesian estimates from the Roll, the extended Roll (MS), and the extended GH (GH) model.

Bayes - MLE	parameters	Roll	MS	GH
Average difference	$c \times 10,000$	0.0000	0.0001	-0.0010
	$\sigma_u \times 10,000$	0.0000	0.0000	-0.0027
	$\lambda_0 \times 10,000$	-	-	0.0052
	$\lambda_1 \times 10,000$	-	-	-0.0021
	P	-	0.0003	-0.0021
	Q	-	0.0000	0.0009

Bayes - MLE	Parameters	Roll	MS	GH
Max abs(difference)	$c \times 10,000$	0.0013	0.0019	0.0272
	$\sigma_u \times 10,000$	0.0013	0.0004	0.0702
	$\lambda_0 \times 10,000$	-	-	0.1223
	$\lambda_1 \times 10,000$	-	-	0.0513
	P	-	0.0074	0.0845
	Q	-	0.0013	0.0381

Table A3. Model comparison (Likelihood ratio test)

This table presents model comparison results from the Roll, and the extended Roll (MS), and the extended GH (GH) models based on the likelihood ratio tests as follows.

$$-2 \ln \left(\frac{\hat{L}_R}{\hat{L}_U} \right) \sim \chi^2_k$$

where \hat{L}_R and \hat{L}_U are the likelihood value under restricted model and unrestricted model, respectively. For example, when we compare the Roll model with the extended GH model, \hat{L}_R and \hat{L}_U are the likelihood value under the Roll model and under the extended GH model, respectively. Since we need to put restrictions on four parameters (P, Q, λ_0 and λ_1) on the extended GH model to obtain the Roll model, the test statistics follows a chi-square distribution with 4 degrees of freedom.

Crit(1%), 6.6349 (Roll-MS), 11.3449 (Roll-GH), 9.2103 (MS-GH)						
Date	Model	Likelihood		Likelihood ratio test		
1-May	Roll	506516.3411	Comparison	LR:Roll-MS	LR:Roll-GH	LR:MS-GH
	MS	507429.8096	Chi-stat	1826.9369	4544.4196	2717.4827
	GH	508788.5509	P-value	0	0	0
2-May	Roll	534907.565	Comparison	LR:Roll-MS	LR:Roll-GH	LR:MS-GH
	MS	536174.3543	Chi-stat	2533.5785	5993.3090	3459.7305
	GH	537904.2195	P-value	0	0	0
3-May	Roll	563875.5491	Comparison	LR:Roll-MS	LR:Roll-GH	LR:MS-GH
	MS	565407.3009	Chi-stat	3063.5037	6233.1780	3169.6743
	GH	566992.1381	P-value	0	0	0
4-May	Roll	480310.5331	Comparison	LR:Roll-MS	LR:Roll-GH	LR:MS-GH
	MS	481533.6496	Chi-stat	2446.2331	4987.4244	2541.1914
	GH	482804.2453	P-value	0	0	0
5-May	Roll	643872.5622	Comparison	LR:Roll-MS	LR:Roll-GH	LR:MS-GH
	MS	645299.3172	Chi-stat	2853.5099	6354.5856	3501.0757
	GH	647049.855	P-value	0	0	0
8-May	Roll	521049.5271	Comparison	LR:Roll-MS	LR:Roll-GH	LR:MS-GH
	MS	523056.4188	Chi-stat	4013.7834	6790.0208	2776.2374
	GH	524444.5375	P-value	0	0	0
9-May	Roll	429310.7187	Comparison	LR:Roll-MS	LR:Roll-GH	LR:MS-GH
	MS	430505.897	Chi-stat	2390.3566	4884.1660	2493.8094
	GH	431752.8017	P-value	0	0	0
10-May	Roll	445413.9822	Comparison	LR:Roll-MS	LR:Roll-GH	LR:MS-GH
	MS	447043.2221	Chi-stat	3258.4798	6198.8750	2940.3953
	GH	448513.4197	P-value	0	0	0
11-May	Roll	498291.7839	Comparison	LR:Roll-MS	LR:Roll-GH	LR:MS-GH
	MS	499815.2659	Chi-stat	3046.9641	5984.7968	2937.8328
	GH	501284.1823	P-value	0	0	0
12-May	Roll	463180.7376	Comparison	LR:Roll-MS	LR:Roll-GH	LR:MS-GH
	MS	464474.9132	Chi-stat	2588.3511	5352.4716	2764.1205
	GH	465856.9734	P-value	0	0	0
15-May	Roll	479958.3703	Comparison	LR:Roll-MS	LR:Roll-GH	LR:MS-GH
	MS	481619.7409	Chi-stat	3322.7412	5761.2219	2438.4807
	GH	482838.9813	P-value	0	0	0
16-May	Roll	488362.0101	Comparison	LR:Roll-MS	LR:Roll-GH	LR:MS-GH

	MS	489909.8219	Chi-stat	3095.6235	5825.5533	2729.9298
	GH	491274.7868	P-value	0	0	0
17-May	Roll	582443.3422	Comparison	LR:Roll-MS	LR:Roll-GH	LR:MS-GH
	MS	583638.2658	Chi-stat	2389.8472	6063.9801	3674.1329
	GH	585475.3323	P-value	0	0	0
18-May	Roll	581842.2541	Comparison	LR:Roll-MS	LR:Roll-GH	LR:MS-GH
	MS	584348.0668	Chi-stat	5011.6255	8264.8027	3253.1771
	GH	585974.6554	P-value	0	0	0
19-May	Roll	362660.0529	Comparison	LR:Roll-MS	LR:Roll-GH	LR:MS-GH
	MS	364184.207	Chi-stat	3048.3083	4902.4966	1854.1883
	GH	365111.3011	P-value	0	0	0
22-May	Roll	391784.1099	Comparison	LR:Roll-MS	LR:Roll-GH	LR:MS-GH
	MS	394046.2345	Chi-stat	4524.2491	6184.3464	1660.0972
	GH	394876.2831	P-value	0	0	0
23-May	Roll	504834.4489	Comparison	LR:Roll-MS	LR:Roll-GH	LR:MS-GH
	MS	507961.0369	Chi-stat	6253.1761	9019.2506	2766.0745
	GH	509344.0742	P-value	0	0	0
24-May	Roll	426820.3463	Comparison	LR:Roll-MS	LR:Roll-GH	LR:MS-GH
	MS	429332.9695	Chi-stat	5025.2465	7617.5436	2592.2971
	GH	430629.1181	P-value	0	0	0
25-May	Roll	368283.5937	Comparison	LR:Roll-MS	LR:Roll-GH	LR:MS-GH
	MS	369811.1244	Chi-stat	3055.0614	4982.7536	1927.6922
	GH	370774.9705	P-value	0	0	0
26-May	Roll	409937.9610	Comparison	LR:Roll-MS	LR:Roll-GH	LR:MS-GH
	MS	411698.1906	Chi-stat	3520.4591	6524.8684	3004.4093
	GH	413200.3952	P-value	0	0	0
29-May	Roll	245069.8893	Comparison	LR:Roll-MS	LR:Roll-GH	LR:MS-GH
	MS	245384.3328	Chi-stat	628.8869	2015.8596	1386.9727
	GH	246077.8191	P-value	0	0	0
30-May	Roll	387333.0538	Comparison	LR:Roll-MS	LR:Roll-GH	LR:MS-GH
	MS	388964.1733	Chi-stat	3262.2390	5358.2592	2096.0202
	GH	390012.1833	P-value	0	0	0
31-May	Roll	410784.406	Comparison	LR:Roll-MS	LR:Roll-GH	LR:MS-GH
	MS	412664.8679	Chi-stat	3760.9238	5602.1671	1841.2433
	GH	413585.4895	P-value	0	0	0
1-Jun	Roll	322725.4681	Comparison	LR:Roll-MS	LR:Roll-GH	LR:MS-GH
	MS	324025.2884	Chi-stat	2599.6405	3893.7146	1294.0740
	GH	324672.3254	P-value	0	0	0
2-Jun	Roll	570025.7323	Comparison	LR:Roll-MS	LR:Roll-GH	LR:MS-GH
	MS	571681.6274	Chi-stat	3311.7902	4866.7338	1554.9435
	GH	572459.0992	P-value	0	0	0
5-Jun	Roll	432138.5773	Comparison	LR:Roll-MS	LR:Roll-GH	LR:MS-GH
	MS	434409.7598	Chi-stat	4542.3650	6720.9511	2178.5861
	GH	435499.0528	P-value	0	0	0
6-Jun	Roll	315554.1838	Comparison	LR:Roll-MS	LR:Roll-GH	LR:MS-GH
	MS	316977.6943	Chi-stat	2847.0210	4228.0255	1381.0045
	GH	317668.1966	P-value	0	0	0
7-Jun	Roll	408143.8464	Comparison	LR:Roll-MS	LR:Roll-GH	LR:MS-GH
	MS	410522.4484	Chi-stat	4757.2040	6898.4437	2141.2397
	GH	411593.0683	P-value	0	0	0
8-Jun	Roll	392998.4378	Comparison	LR:Roll-MS	LR:Roll-GH	LR:MS-GH
	MS	394881.2157	Chi-stat	3765.5559	5779.1010	2013.5452
	GH	395887.9883	P-value	0	0	0
9-Jun	Roll	389712.6362	Comparison	LR:Roll-MS	LR:Roll-GH	LR:MS-GH
	MS	391565.2274	Chi-stat	3705.1824	5361.7774	1656.5950
	GH	392393.5249	P-value	0	0	0
12-Jun	Roll	517206.8955	Comparison	LR:Roll-MS	LR:Roll-GH	LR:MS-GH

	MS	519606.3378	Chi-stat	4798.8845	8008.6417	3209.7572
	GH	521211.2164	P-value	0	0	0
13-Jun	Roll	489502.5198	Comparison	LR:Roll-MS	LR:Roll-GH	LR:MS-GH
	MS	492309.1285	Chi-stat	5613.2175	8273.0244	2659.8069
	GH	493639.032	P-value	0	0	0
14-Jun	Roll	511532.4208	Comparison	LR:Roll-MS	LR:Roll-GH	LR:MS-GH
	MS	513162.2615	Chi-stat	3259.6815	5427.8531	2168.1716
	GH	514246.3473	P-value	0	0	0
15-Jun	Roll	867118.8519	Comparison	LR:Roll-MS	LR:Roll-GH	LR:MS-GH
	MS	870552.3898	Chi-stat	6867.0758	12740.2098	5873.1340
	GH	873488.9568	P-value	0	0	0
16-Jun	Roll	530716.4036	Comparison	LR:Roll-MS	LR:Roll-GH	LR:MS-GH
	MS	533219.1178	Chi-stat	5005.4283	7886.3863	2880.9580
	GH	534659.5968	P-value	0	0	0
19-Jun	Roll	474641.9255	Comparison	LR:Roll-MS	LR:Roll-GH	LR:MS-GH
	MS	476240.678	Chi-stat	3197.5050	3469.1268	271.6218
	GH	476376.4889	P-value	0	0	0
20-Jun	Roll	519765.9536	Comparison	LR:Roll-MS	LR:Roll-GH	LR:MS-GH
	MS	520691.8947	Chi-stat	1851.8821	5246.3840	3394.5018
	GH	522389.1456	P-value	0	0	0
21-Jun	Roll	369354.6134	Comparison	LR:Roll-MS	LR:Roll-GH	LR:MS-GH
	MS	370201.8094	Chi-stat	1694.3920	3876.7641	2182.3721
	GH	371292.9955	P-value	0	0	0
22-Jun	Roll	444442.935	Comparison	LR:Roll-MS	LR:Roll-GH	LR:MS-GH
	MS	444883.4025	Chi-stat	880.9349	3413.8757	2532.9408
	GH	446149.8729	P-value	0	0	0
23-Jun	Roll	1374533.738	Comparison	LR:Roll-MS	LR:Roll-GH	LR:MS-GH
	MS	1386969.649	Chi-stat	24871.8216	29075.2245	4203.4029
	GH	1389071.351	P-value	0	0	0
26-Jun	Roll	683033.9206	Comparison	LR:Roll-MS	LR:Roll-GH	LR:MS-GH
	MS	684608.0586	Chi-stat	3148.2760	5604.7667	2456.4907
	GH	685836.304	P-value	0	0	0
27-Jun	Roll	480307.2243	Comparison	LR:Roll-MS	LR:Roll-GH	LR:MS-GH
	MS	481121.4758	Chi-stat	1628.5031	4280.9591	2652.4561
	GH	482447.7039	P-value	0	0	0
28-Jun	Roll	449722.4166	Comparison	LR:Roll-MS	LR:Roll-GH	LR:MS-GH
	MS	450602.4876	Chi-stat	1760.1420	4875.4327	3115.2907
	GH	452160.133	P-value	0	0	0
29-Jun	Roll	480259.7110	Comparison	LR:Roll-MS	LR:Roll-GH	LR:MS-GH
	MS	481791.8537	Chi-stat	3064.2856	6243.7616	3179.4760
	GH	483381.5918	P-value	0	0	0

Appendix A

A. Bayesian Estimation of the empirical market microstructure models

We proceed first by discussing briefly Hasbrouck's Gibbs sampling algorithm for the Roll model followed by the estimation algorithms we propose for the case of the extended Roll and Glosten and Harris models with autocorrelated trade direction indicators.

A.1 Hasbrouck (2004)

To facilitate the explanations to follow, we reproduce the Roll model, equation (1) in the text:

$$p_t = m_t + cq_t$$

$$m_t = m_{t-1} + u_t, \quad u_t \sim N(0, \sigma_u^2)$$

where p_t is the log transaction price, m_t is the efficient price, q_t is the independent trade direction indicator, and c is the (log) half bid-ask spread. To estimate this model, we use Hasbrouck (2004)'s codes downloaded from his website.

Hasbrouck (2004) draws c, σ_u^2 , and $q(\equiv [q_1, \dots, q_T])$ repeatedly from the posterior conditional density as follows given data $(p \equiv [p_1, \dots, p_T])$:

- Draw $q^{(1)}$ from $f(q_1, \dots, q_T | c^{(0)}, \sigma_u^{(0)}, p)$
- Draw $c^{(1)}$ from $f(c | \sigma_u^{(0)}, q^{(1)}, p)$
- Draw $\sigma_u^{(1)}$ from $f(\sigma_u | c^{(1)}, q^{(1)}, p)$

The final output is $\{c^{(j)}, \sigma_u^{(j)}, q^{(j)}\}$ for $j = \text{number of simulations}$.

A.1.1 Exact forms of conditional posterior densities

The Roll model can be expressed in regression form as $Y = Xc + u$, $E(uu') = \sigma_u^2 I_{T-1}$. In the present setup, $Y = [\Delta p_2, \dots, \Delta p_T]$, $X = [\Delta q_2, \dots, \Delta q_T]$, and $u = [u_2, \dots, u_T]$. By using conjugate prior distributions, the conditional posterior distributions for the standard regression parameters are given as follows.

- i. **Log half spread (c):**

- Prior distribution : $c \sim N(\mu_c^{prior}, \Omega_c^{prior})$
- Posterior distribution: $c | Y, X \sim N(\mu_c^{posterior}, \Omega_c^{posterior})$

where $\mu_c^{posterior} = Dd, \Omega_c^{posterior} = D$

$$D^{-1} = X' \Omega_u^{-1} X + (\Omega_u^{prior})^{-1} \quad \text{and} \quad d = X' \Omega_u^{-1} Y + (\Omega_u^{prior})^{-1} \mu_u^{prior}$$

We impose a non-informative prior for c by assuming a small value for $\mu_c^{prior} (10^{-6})$

and large number for $\Omega_c^{prior} (10^6)$. As economic theory dictates the half-spread is positive, Hasbrouck uses a truncated normal density to ensure a $c > 0$.

In this normal linear regression model, the conjugate prior distribution for the variance parameter is the inverted gamma distribution.

ii. The variance parameter (σ_u^2):

- Prior distribution: $\frac{1}{\sigma_u^2} | c \square \Gamma\left(\frac{\nu_0}{2}, \frac{\delta_0}{2}\right)$
- Posterior distribution: $\frac{1}{\sigma_u^2} | c, Y, X \square \Gamma\left(\frac{\nu_1}{2}, \frac{\delta_1}{2}\right)$

$$\text{where } \nu_0 = \nu_1 + T - 2, \delta_0 = \delta_1 = \delta_0 (Y - \bar{X})' c (Y - \bar{X})$$

iii. The independent trade direction indicator

First, we express the joint distribution of $q (\equiv [q_1, \dots, q_T])$ using Bayes' theorem and subsequently simplify as in this case $\Pr(q) = 0.5$, and $f(p)$ does not depend on q . For economy of notation, parameters that are given will be dropped from the explicit conditioning set.

$$pr(q | p) = f(p | q) \times pr(q) \times \frac{1}{f(p)} \propto f(p | q)$$

Hasbrouck uses a single-move Gibbs sampling algorithm to draw q_t sequentially as follows.

- Draw q_1^* from $\Pr(q_1 | p, q_2, q_3, \dots, q_T)$
- Draw q_2^* from $\Pr(q_2 | p, q_1^*, q_3, \dots, q_T)$
- ⋮
- Draw q_T^* from $\Pr(q_T | p, q_1^*, q_2^*, \dots, q_{T-1}^*)$

where q_t^* is the newly drawn value of q_t from those remaining after the previous draw. To complete this algorithm, Hasbrouck derives the conditional distribution $pr(q_t | p_t, m_{t-1}, m_{t+1})$ using Bayes' theorem, simplifying it as neither $pr(q_t | m_{t-1}, m_{t+1})$ nor $f(p_t | m_{t-1}, m_{t+1})$ depend on q .

$$pr(q_t | p_t, m_{t-1}, m_{t+1}) = \frac{f(p_t | q_t, m_{t-1}, m_{t+1}) \times pr(q_t | m_{t-1}, m_{t+1})}{f(p_t | m_{t-1}, m_{t+1})} \propto f(p_t | q_t, m_{t-1}, m_{t+1})$$

Hasbrouck demonstrates that $f(p_t | q_t, m_{t-1}, m_{t+1})$ follows a normal distribution $(\phi(\mu_x, \sigma_x, p_t - cq_t) = \frac{1}{\sqrt{2\pi\sigma_x^2}} \exp\left(-\frac{((p_t - cq_t) - \mu_x)^2}{2\sigma_x^2}\right))$ and derives posterior densities for three different scenarios. The non-normalized probabilities of a buy and a sell order are determined after evaluating each case at $q_t = +1$ and $q_t = -1$, respectively. The normalized probability of a buy for the three different possibilities is given as follows.

- For $t=1$,

$$pr(q_1 = 1 | p, q_2, q_3, \dots, q_T) = \frac{\phi(0, \sigma_u, m_2 - p_1 + c)}{\phi(0, \sigma_u, m_2 - p_1 + c) + \phi(0, \sigma_u, m_2 - p_1 - c)},$$

where $m_t = p_t - cq_t$

- For $t=2, \dots, T-1$,

$$pr(q_t = 1 | p, q_1, \dots, q_{t-1}, q_{t+1}, \dots, q_T) = \frac{\phi\left(\frac{1}{2}(m_{t-1} + m_{t+1}), \frac{\sigma_u}{\sqrt{2}}, p_t - c\right)}{\phi\left(\frac{1}{2}(m_{t-1} + m_{t+1}), \frac{\sigma_u}{\sqrt{2}}, p_t - c\right) + \phi\left(\frac{1}{2}(m_{t-1} + m_{t+1}), \frac{\sigma_u}{\sqrt{2}}, c + p_t\right)}$$

- For $t=T$,

$$pr(q_T = 1 | p, q_1, q_2, q_3, \dots, q_{T-1}) = \frac{\phi(0, \sigma_u, p_T - c - m_{T-1})}{\phi(0, \sigma_u, p_T - c - m_{T-1}) + \phi(0, \sigma_u, p_T + c - m_{T-1})}$$

For each scenario, the Hasbrouck (2004) algorithm draws a random number from the uniform distribution (0,1). If the random number is lower than the normalized probability of a buy it chooses $q_1 = +1$ (and otherwise, $q_1 = -1$).

A.2 The extended Roll model with an autocorrelated trade direction indicator

To facilitate the explanations to follow, we first reproduce the extended Roll model in the text:

$$\Delta p_t = c \Delta q_t + u_t, u_t \sim N(0, \sigma_u^2)$$

where $q_t \in \{1, -1\}$, $P = \text{pr}[q_t = 1 | q_{t-1} = 1]$ and $Q = \text{pr}[q_t = -1 | q_{t-1} = -1]$

The above model extends the Roll model (Hasbrouck's algorithm) by incorporating a single move Gibbs sampling algorithm to simulate the autocorrelated and latent trade direction indicator along with its transition probabilities. In sum, the estimation algorithm consists of the following five steps.

- Draw $q^{(1)}$ from $f(q_1, \dots, q_T | c^{(0)}, P^{(0)}, Q^{(0)}, \sigma_u^{(0)}, p)$
- Draw $c^{(1)}$ from $f(c | \sigma_u^{(0)}, q^{(1)}, p)$
- Draw $\sigma_u^{(1)}$ from $f(\sigma_u | c^{(1)}, q^{(1)}, p)$
- Draw $P^{(1)}$ from $f(P | Q^{(0)}, q^{(1)}, p)$
- Draw $Q^{(1)}$ from $f(Q | P^{(1)}, q^{(1)}, p)$

The final output is $\{c^{(j)}, \sigma_u^{(j)}, P^{(j)}, Q^{(j)}, q^{(j)}\}$ for $j = \text{number of simulations}$.

For the half spread (c) and the variance parameter (σ_u^2), we still adopt Hasbrouck's algorithms explained in A.1.

i. The autocorrelated trade direction indicator

First, after suppressing the conditioning on the parameters, the conditional distribution of q_t is derived via Bayes' rule as follows:

$$\text{pr}(q_t | q_{\neq t}, Y) = \frac{f(Y | q) \text{pr}(q_t | q_{\neq t})}{f(Y | q_{\neq t})} \propto f(Y | q) \text{pr}(q_t | q_{\neq t})$$

where $Y_t = (\Delta p_2, \dots, \Delta p_t), Y = Y_T$, and $q_{\neq t} = \{q_1, \dots, q_{t-1}, q_{t+1}, \dots, q_T\}$,

The first term in the above equation is:

$$\begin{aligned} f(Y | q) &= f(\Delta p_2 | \Delta p_1, q) \cdots f(\Delta p_T | Y_{T-1}, q) \\ &= f(\Delta p_2 | q_2, q_1) \cdots f(\Delta p_t | q_t, q_{t-1}) \cdots f(\Delta p_T | q_T, q_{T-1}) \\ &\propto f(\Delta p_t | q_t, q_{t-1}) f(\Delta p_{t+1} | q_{t+1}, q_t) \end{aligned}$$

The second line of the above equation arises from the fact that the likelihood function of $\Delta p_t (t=1, \dots, T)$ depends on the past state variables, q_{t-1}, q_t , while the third follows from the fact that all terms except for $f(\Delta p_t | q_t, q_{t-1})$ and $f(\Delta p_{t+1} | q_{t+1}, q_t)$ are constant, since we are concerned with the probability of q_t conditional on Y and all the other q_t 's.

The second term is given by:

$$\begin{aligned}
pr(q_t | q_{\neq t}) &= pr(q_t | q_1, \dots, q_{t-1}, q_{t+1}, \dots, q_T) \\
&= \frac{pr(q_{t+1}, \dots, q_T | q_1, \dots, q_t) pr(q_t | q_1, \dots, q_{t-1})}{pr(q_{t+1}, \dots, q_T | q_1, \dots, q_{t-1})} \\
&\propto pr(q_{t+1}, \dots, q_T | q_1, \dots, q_t) pr(q_t | q_1, \dots, q_{t-1}) \\
&= pr(q_{t+1} | q_1, \dots, q_t) pr(q_{t+2} | q_1, \dots, q_{t+1}), \dots, pr(q_T | q_1, \dots, q_{T-1}) pr(q_t | q_1, \dots, q_{t-1}) \\
&= pr(q_{t+1} | q_t) pr(q_{t+2} | q_{t+1}), \dots, pr(q_T | q_{T-1}) pr(q_t | q_{t-1}) \\
&\propto pr(q_{t+1} | q_t) pr(q_t | q_{t-1})
\end{aligned}$$

Applying Bayes' rule to the second line, and the Markov property of state variables to the fifth line and combining, we obtain the final conditional distribution.

$$pr(q_t | q_{\neq t}, Y) \propto f(Y | q) pr(q_t | q_{\neq t}) = f(\Delta p_t | q_t, q_{t-1}) f(\Delta p_{t+1} | q_{t+1}, q_t) pr(q_{t+1} | q_t) pr(q_t | q_{t-1})$$

Let $P_0 = pr(q_t = -1 | q_{\neq t}, Y)$ and $P_1 = pr(q_t = 1 | q_{\neq t}, Y)$. These are un-normalized probabilities of a sell and a buy order, respectively. By using two values, we obtain the following normalized probabilities:

$$Pr_0 = \frac{P_0}{P_0 + P_1}$$

If the normalized probability of a sell (Pr_0) is higher (lower) than a value from the uniform distribution (0,1), we set $q_t = -1$ (+1). Specifically, the simulation algorithm can be stated as follows.

- For $t = 0$,

We use the unconditional probability to determine the direction of q_0

$$pr[q_0 = 1] = \frac{1-Q}{2-P-Q}$$

If $pr[q_0 = 1]$ is higher than a draw from uniform distribution [0,1], then $q_0 = 1$.

- For $t = 1, \dots, T-1$,

$$pr(q_t | q_{\neq t}, Y) \propto f(\Delta p_t | q_t, q_{t-1}) f(\Delta p_{t+1} | q_{t+1}, q_t) pr(q_{t+1} | q_t) pr(q_t | q_{t-1})$$

$$\text{where } pr(q_t = -1 | q_{\neq t}, Y) \propto \exp \left\{ -\frac{1}{2\sigma^2} \left(((\Delta p_t - c(-1 - q_{t-1}))^2 + (\Delta p_{t+1} - c(q_{t+1} + 1))^2 \right) \right\} \\ \cdot pr(q_{t+1} | q_t = -1) \cdot pr(q_t = -1 | q_{t-1})$$

$$pr(q_t = 1 | q_{\neq t}, Y) \propto \exp \left\{ -\frac{1}{2\sigma^2} \left(((\Delta p_t - c(1 - q_{t-1}))^2 + (\Delta p_{t+1} - c(q_{t+1} - 1))^2 \right) \right\} \\ \cdot pr(q_{t+1} | q_t = 1) \cdot pr(q_t = 1 | q_{t-1})$$

- For $t = T$,

$$pr(q_T | q_{\neq T}, Y) \propto f(\Delta p_T | q_T, q_{T-1}) pr(q_T | q_{T-1})$$

$$\text{where } pr(q_T = -1 | q_{\neq T}, Y) \propto \exp \left\{ -\frac{1}{2\sigma_u^2} ((\Delta p_T - c(-1 - q_{T-1}))^2 \right\} pr(q_T = -1 | q_{T-1})$$

$$pr(q_T = 1 | q_{\neq T}, Y) \propto \exp \left\{ -\frac{1}{2\sigma_u^2} ((\Delta p_T - c(1 - q_{T-1}))^2 \right\} pr(q_T = 1 | q_{T-1})$$

ii. Transition probabilities:

Finally, we are required to estimate the two transition probabilities P and Q . Following the discussion contained in Chapter 9 of Kim and Nelson (1999), we use the beta distribution as follows:

- Independent prior distribution :

$$P \sim beta(u_{11}, u_{1-1}) = P^{u_{11}-1} (1-P)^{u_{1-1}-1}$$

$$Q \sim beta(u_{-1-1}, u_{-11}) = Q^{u_{-1-1}-1} (1-Q)^{u_{-11}-1}$$

where u_{ij} ($i, j = -1, 1$) are known parameters of the priors.

- Posterior distribution :

$$P | q \square beta(u_{1-1} + n_{-1}, u_{-11} + n_{-1})$$

$$Q | q \square beta(u_{-1-1} + n_{-1}, u_{-11} + n_{-1})$$

where n_{ij} refers to the transitions from state i to j , which can be easily counted for given q .

A3. The extended Glosten and Harris Model

To facilitate the explanations to follow, we reproduce the extended Glosten and Harris model in the text:

$$\Delta p_t = c \Delta q_t + (\lambda_0 + \lambda_1 \sqrt{V_t}) (q_t - ((P - Q) + (P + Q - 1)q_{t-1})) + u_t, \quad u_t \sim N(0, \sigma_u^2)$$

In this model, we have two extra parameters (λ_0 and λ_1) and two transition probabilities (P and Q) appearing in the main regression. Therefore, the conditional posterior densities for the transition probabilities parameters do not follow any known distributions. Therefore the Gibbs sampling estimation algorithm as employed in the previous section is not feasible to estimate these parameters. To overcome this issue, we adopt a variant of the tailored Random-Walk Metropolis-Hastings Algorithm developed by Chib and Ramamurthy (2010).

Specifically, we draw $c, \lambda_0, \lambda_1, P, Q, \sigma_u$, and q repeatedly as follows. First, the parameters and latent trade direction indicators are set equal to some arbitrary values. Denoting these initial values as $\{[c^{(0)}, \lambda_0^{(0)}, \lambda_1^{(0)}, P^{(0)}, Q^{(0)}], \sigma_u^{(0)}, q^{(0)}\}$, the first step is represented as follows.

- Draw $q^{(1)}$ from $f(q | [c^{(0)}, \lambda_0^{(0)}, \lambda_1^{(0)}, P^{(0)}, Q^{(0)}], \sigma_u^{(0)}, Y)$
- Draw $[c^{(1)}, \lambda_0^{(1)}, \lambda_1^{(1)}, P^{(1)}, Q^{(1)}]$ from $f(c, \lambda_0, \lambda_1, P, Q | \sigma_u^{(0)}, q^{(1)}, Y)$
- Draw $\sigma_u^{(1)}$ from $f(\sigma_u | [c^{(1)}, \lambda_0^{(1)}, \lambda_1^{(1)}, P^{(1)}, Q^{(1)}], q^{(1)}, Y)$

By repeating this procedure many times, we generate a sequence of draws of unknowns for $j = 1, \dots, n$. The Gibbs principle demonstrates that the limiting distribution of the n^{th} draw after burn-in samples (as $n \rightarrow \infty$) is $f([c, \lambda_0, \lambda_1, P, Q], \sigma_u, q | Y)$, the desired posterior, and the limiting draw for any parameter is distributed as the corresponding marginal posterior. The details for Bayesian algorithms are presented below.

i. The autocorrelated trade direction indicator

Once we suppress the conditioning on the parameters, the conditional distribution of q_t is derived via Bayes' rule following the procedure outlined in A.2.

$$pr(q_t | q_{\neq t}, Y) \propto f(Y | q) pr(q_t | q_{\neq t}) \propto f(\Delta p_t | q_t, q_{t-1}) f(\Delta p_{t+1} | q_{t+1}, q_t) pr(q_{t+1} | q_t) pr(q_t | q_{t-1})$$

Define $P_0 = pr(q_t = -1 | q_{\neq t}, Y)$ and $P_1 = pr(q_t = 1 | q_{\neq t}, Y)$ as the non-normalized probabilities of a sell and a buy trade. By using these two values, we obtain the following normalized probabilities for $q_t = -1$.

$$\Pr_0 = \frac{P_0}{P_0 + P_1}$$

If the normalized probability of a sell (\Pr_0) is higher (lower) than a value from the uniform distribution (0,1), we set $q_t = -1$ (+1). Specifically, the simulation algorithm can be stated as follows.

Specifically, the simulation algorithm can be stated as follows.

- For $t = 0$,

We use the unconditional probability to determine the q_0 .

$$pr[q_0 = 1] = \frac{1-Q}{2-P-Q}$$

If $pr[q_0 = 1]$ is higher than a draw from uniform distribution [0,1], then $q_0 = 1$.

- For $t = 1, \dots, T-1$,

$$pr(q_t | q_{\neq t}, Y) \propto f(\Delta p_t | q_t, q_{t-1}) f(\Delta p_{t+1} | q_{t+1}, q_t) pr(q_{t+1} | q_t) pr(q_t | q_{t-1})$$

$$\text{where } pr(q_t = -1 | q_{\neq t}, Y) \propto \exp \left\{ -\frac{1}{2\sigma_u^2} \left[\left((\Delta p_t - c(-1 - q_{t-1})) + (\lambda_0 + \lambda_1 \sqrt{V_t}) \times (1 + \mu + \rho q_{t-1}) \right)^2 + \left(\Delta p_{t+1} - c(q_{t+1} + 1) - (\lambda_0 + \lambda_1 \sqrt{V_{t+1}}) \times (q_{t+1} - \mu + \rho) \right)^2 \right] \right\}$$

$$\bullet pr(q_{t+1} | q_t = -1) \times pr(q_t = -1 | q_{t-1})$$

$$pr(q_t = 1 | q_{\neq t}, Y) \propto \exp \left\{ -\frac{1}{2\sigma_u^2} \left[\left((\Delta p_t - c(1 - q_{t-1})) + (\lambda_0 + \lambda_1 \sqrt{V_t}) \times (-1 + \mu + \rho q_{t-1}) \right)^2 + \left(\Delta p_{t+1} - c(q_{t+1} - 1) - (\lambda_0 + \lambda_1 \sqrt{V_{t+1}}) \times (q_{t+1} - \mu - \rho) \right)^2 \right] \right\}$$

$$\bullet pr(q_{t+1} | q_t = 1) \times pr(q_t = 1 | q_{t-1})$$

where $\mu = P - Q$ and $\rho = P + Q - 1$

- For $t = T$,

$$pr(q_T | q_{\neq T}, Y) \propto pr(\Delta p_T | q_T, q_{T-1}) pr(q_T | q_{T-1})$$

$$\text{where } pr(q_T = -1 | q_{\neq T}, Y) \propto \exp \left\{ -\frac{1}{2\sigma_u^2} \left((\Delta p_T - c(-1 - q_{T-1})) + (\lambda_0 + \lambda_1 \sqrt{V_T}) \times (1 + \mu + \rho q_{T-1}) \right)^2 \right\}$$

$$\cdot p(q_T = -1 | q_{T-1})$$

$$P_1 = p(q_T = 1 | q_{\neq T}, Y) \propto \exp \left\{ -\frac{1}{2\sigma_u^2} \left((\Delta p_T - c(1 - q_{T-1})) + (\lambda_0 + \lambda_1 \sqrt{V_T}) \times (-1 + \mu + \rho q_{T-1}) \right)^2 \right\}$$

$$\cdot p(q_T = 1 | q_{T-1})$$

ii. The mean parameters $(c, \lambda_0, \lambda_1, P, Q)$

We use the tailored random walk Metropolis Hastings algorithm to draw $\theta = (c, \lambda_0, \lambda_1, P, Q)$ given other model parameters and the latent variables (q) with the positivity restriction on ($c > 0$)

In order to compute an acceptance/rejection probability for the Metropolis Hastings algorithm, we need to derive the joint conditional posterior density of $\theta = (c, \lambda_0, \lambda_1, P, Q)$.

- Prior distribution of $\theta = (c, \lambda_0, \lambda_1, P, Q)$:

We assume independent prior distributions for the following parameters.

a. Multivariate normal density prior for $\beta = (c, \lambda_0, \lambda_1)$

$$\beta \sim N(\beta_0, \Sigma_0) = (2\pi)^{-\frac{3}{2}} |\Sigma_0|^{-\frac{1}{2}} e^{-\frac{1}{2}(\beta - \beta_0)' \Sigma_0^{-1} (\beta - \beta_0)}$$

b. Beta density prior for P and Q

$$: beta(P, Q) = P^{u_{1,1}-1} (1-P)^{u_{1,-1}-1} Q^{u_{-1,-1}-1} (1-Q)^{u_{-1,1}-1}$$

Therefore, the joint prior density for $\theta = (c, \lambda_0, \lambda_1, P, Q)$ is as follows.

$$P^{u_{11}-1}Q^{u_{-11}-1}(1-Q)^{u_{-11}-1}(1-P)^{u_{1-1}-1} \times (2\pi)^{-\frac{3}{2}}|\Sigma_0|^{-\frac{1}{2}}e^{-\frac{1}{2}(\beta-\beta_0)'\Sigma_0^{-1}(\beta-\beta_0)}$$

- Conditional likelihood function given q

The conditional likelihood function $L(c, \lambda_0, \lambda_1, P, Q | q, Y)$ of the extended Glosten and Harris (1988) model is formed by suppressing the conditioning on all the parameters and data except for q and Y as follows.

$$L(c, \lambda_0, \lambda_1, P, Q | q, Y) = f(Y | q) pr(q)$$

$$\text{Where } f(Y | q) = f(y_1 | q_1, q_0, \tilde{y}_0) f(y_2 | q_2, q_1, \tilde{y}_1) \cdots f(y_T | q_T, q_{T-1}, \tilde{y}_{T-1})$$

$$f(q) = f(q_1 | q_0) f(q_2 | q_1) \cdots f(q_T | q_{T-1}) \text{ and } \tilde{y}_{t-1} = \{y_1, y_2, \dots, y_{t-1}\}$$

We can express the above likelihood function in the following compact form.

$$L(c, \lambda_0, \lambda_1, P, Q | q, Y) = f_{ij}(1) \times \cdots \times f_{ij}(T) \times P^{n_{11}} Q^{n_{-11}} (1-Q)^{n_{-11}} (1-P)^{n_{1-1}}$$

where $i, j = \{1, -1\}$ and $n_{i,j}$ is the total number of transitions from state $q_{t-1} = i$ to $q_t = j$, for $t=1, 2, \dots, T$. And $f_{ij}(t) = f(\Delta p_t | q_t = j, q_{t-1} = i, \tilde{y}_{t-1})$

$$= \frac{1}{\sqrt{2\pi\sigma_u^2}} \exp \left\{ -\frac{1}{2\sigma_u^2} \left(\Delta p_t - c(q_t^j - q_{t-1}^i) - (\lambda_0 + \lambda_1 \sqrt{V_t}) (q_t^j - (\mu + \rho q_{t-1}^i)) \right)^2 \right\}$$

- Conditional Posterior density of $\theta = (c, \lambda_0, \lambda_1, P, Q)$ given q

By multiplying the joint prior density by the conditional likelihood function, we obtain the following conditional posterior density $f(c, \lambda_0, \lambda_1, P, Q | q, Y)$.

$$f(c, \lambda_0, \lambda_1, P, Q | q, Y) \propto f_{ij}(1) \times \cdots \times f_{ij}(T) \times P^{u_{11}+n_{11}-1} Q^{u_{-11}+n_{-11}-1} (1-Q)^{u_{-11}+n_{-11}-1} (1-P)^{u_{1-1}+n_{1-1}-1} \times (2\pi)^{-\frac{3}{2}} |\Sigma_0|^{-\frac{1}{2}} e^{-\frac{1}{2}(\beta-\beta_0)'\Sigma_0^{-1}(\beta-\beta_0)}$$

- Joint proposal density $\theta = (c, \lambda_0, \lambda_1, P, Q)$

We follow the procedure underpinning the joint proposal density of the tailored Random-Walk Metropolis-Hastings Algorithm developed by Chib and Ramamurthy (2010) as follows.

a. We first maximize the log conditional posterior density using a simulated annealing algorithm or another robust maximization algorithm (e.g. fminsearch in Matlab) to obtain maximum posterior estimates $\theta^* = (c^*, \lambda_0^*, \lambda_1^*, P^*, Q^*)$ and corresponding variance estimate $Var(\theta^*)$. Denote the old (new) parameter value $\theta^{old}(\theta^{new})$ in the MCMC iteration.²¹

b. We simulate a new candidate θ^{new} using the following proposal density, (denoted as $q^*(\theta^{new} | \cdot)$).

Multivariate t -density ($q^*(\theta^{new} | \theta^*, Var(\theta^*), nu)$).

$$\theta^{new} = MVT(\theta^*, Var(\theta^*), nu)$$

where nu is the degree of freedom parameter, and will be set to obtain 20%-50% of acceptance ratio for θ^{new} defined below.

Note: if θ^{new} satisfies the several restrictions on θ (e.g. non-negativity restrictions for c, P, Q) then we proceed to the next step. If that is not the case, we set $\theta = \theta^{old}$ and terminate the draw at this point.

c. We compute the following ratio to accept or reject the proposed value for θ^{new} .

$$\alpha_\theta = \frac{f(\theta^{new} | \tilde{q}_T) \times q^*(\theta^{old} | \cdot)}{f(\theta^{old} | \tilde{q}_T) \times q^*(\theta^{new} | \cdot)}$$

To implement the accept-reject step, we draw a uniform random variable, $U \sim U[0,1]$, and set $\theta = \theta^{new}$ if $U < \alpha_\theta$ and $\theta = \theta^{old}$ if $U > \alpha_\theta$.

²¹ In the new Tailored MH algorithms, in each step of MCMC, we estimate the mode and variance of the proposal densities by maximizing the log posterior densities of all parameters using simulated annealing or Nelder-Mead simplex algorithm.

iv. The variance parameter (σ_u^2):

We need to express first the Glosten and Harris (1988) model in the following regression format.

$$\Delta p_t = \begin{bmatrix} q_t - q_{t-1}, -\mu + q_t - \rho q_{t-1}, q_t \sqrt{V_t} - \mu \sqrt{V_t} - \rho q_{t-1} \sqrt{V_t} \end{bmatrix} \begin{bmatrix} c \\ \lambda_0 \\ \lambda_1 \end{bmatrix} + u_t$$

In matrix notation,

$$y_t = X_t \beta + u_t, u_t \sim N(0, \sigma_u^2)$$

$$\text{where } y_t = \Delta p_t, X_t = \begin{bmatrix} q_t - q_{t-1} \\ -\mu + q_t - \rho q_{t-1} \\ q_t \sqrt{V_t} - \mu \sqrt{V_t} - \rho q_{t-1} \sqrt{V_t} \end{bmatrix}, \beta = \begin{bmatrix} c \\ \lambda_0 \\ \lambda_1 \end{bmatrix}$$

Based on this notation, we can express the conditional posterior distribution for σ_u^2 as follows.

- Prior distribution: $\frac{1}{\sigma_u^2} | \theta \sim \Gamma\left(\frac{\nu_0}{2}, \frac{\delta_0}{2}\right)$
- Posterior distribution: $\frac{1}{\sigma_u^2} | \theta, Y, X \sim \Gamma\left(\frac{\nu_1}{2}, \frac{\delta_1}{2}\right)$

$$\text{where } \nu_1 = \nu_0 + T - 2, Y_1 = Y_2 - [Y_T, X], \delta_1 = \delta_0 + (Y_1' X \beta)' (Y_1 - X \beta)$$

Appendix B

B. MCMC convergence diagnostics

In any MCMC estimation, it is crucial to determine the convergence of the chain to conduct a correct statistical inference. In this paper, as a diagnostic to check the convergence of our MCMC algorithm, we compute and report the effective sample size based on the inefficiency factors and the p-value of Geweke's convergence diagnostics test for the model parameters. Specifically, we start all estimations with 100,000 burn-in period and 250,000 total numbers of iterations and increase these numbers by 10,000 until the convergence criteria for both (explained below) are satisfied simultaneously for all parameters.

B.1 Geweke's convergence diagnostic (CD)

The idea of Geweke's diagnostic is simple and mimics the two-sample test of means. First we set the total number of iterations (n), the burn-in period (n_0), and the rest of iterations (n_1) (i.e., $n = n_0 + n_1$). Then divide n_1 into three periods (e.g., $n_1 = n_A + n_B + n_C$). Specifically, we set the first 40% (n_A), the second 20% (n_B), and the last 40% (n_C) as three sub-periods. And if the mean of the first 40% is not significantly different from that of the last 40%, then we conclude the target distribution converged somewhere in the first 40% of the chain.

More formally, we compute Geweke's CD as follows.

$$CD = \left(\hat{\theta}_{n_A} - \hat{\theta}_{n_C} \right) / \left(\frac{\hat{\sigma}_A}{\sqrt{n_A}} + \frac{\hat{\sigma}_C}{\sqrt{n_C}} \right)$$

where $\hat{\theta}_{n_A}, \hat{\theta}_{n_B}, \hat{\theta}_{n_C}$ ($\hat{\sigma}_A, \hat{\sigma}_B, \hat{\sigma}_C$) are the sample means (standard deviation) of each sub-period. Based on the Geweke's CD, we compute Geweke's p-value at 0.05 significance level to test if the means of the first and the last samples are same.

$$Geweke's\ p = 2 \times [1 - \Phi(|CD|)]$$

where $\Phi(\cdot)$ is the cumulative density function of the standard normal distribution. If Geweke's p-value is less than 0.05, we interpret the burn-in period is too small and we can't

guarantee the convergence of the chain. In general, as Geweke's p-value is close to 1, we have more efficient samples.

B.2. Inefficiency factor and effective sample size

The inefficiency factor, as proposed by Kim, Shephard, Chib (1998), is defined as $1 + 2 \sum_{k=1}^{\infty} \rho(k)$ where $\rho(k)$ is the k^{th} order autocorrelation coefficient and measures how well the MCMC sequence mixes. In this paper, we estimate it as $1 + (2 \times 200) / (200 - 1) \sum_{j=1}^{200} K(j/B) \hat{\rho}(j)$ where $\hat{\rho}(j)$ is the j^{th} order sample autocorrelation coefficient of the MCMC draws and $K(\cdot)$ stands for the Parzen kernel. A value of 1 indicates that the MCMC draws are uncorrelated with a good mixing, while large values indicate a slow mixing. The effective sample size is computed as the ratio of the number of iterations after the burn-in period to the inefficiency factor and should be larger than 1000 for all parameters to guarantee sufficient number of the MCMC draws.

Appendix C

C. Maximum Likelihood Estimation (MLE) methods of the empirical market microstructure models

The empirical market microstructure models employed in this paper imply that we can interpret them as a regime switching model. Based on the Hamilton filter, we obtain a likelihood function and subsequently use MLE methods for estimation (see chapter 4 of Kim and Nelson (1999) for more details).

As an illustration, we demonstrate how to construct the likelihood function for the Glosten and Harris model with autocorrelated q_t . This model implies that:

$$\Delta p_t = c\Delta q_t + (\lambda_0 + \lambda_1 \sqrt{V_t}) (q_t - ((P-Q) + (P+Q-1)q_{t-1})) + u_t, \quad u_t \sim N(0, \sigma_u^2)$$

where p_t is the log transaction price, q_t is the trade direction indicator with transition probabilities $P = pr(q_t = 1 | q_{t-1} = 1)$ and $Q = pr(q_t = -1 | q_{t-1} = -1)$.

On this basis, we interpret this form of the Glosten and Harris model with autocorrelated q_t as a standard regime switching model. The likelihood function $L(c, \lambda_0, \lambda_1, P, Q | \Delta p_2, \dots, \Delta p_T)$ of the extended Glosten and Harris (1988) model is formed by suppressing the conditioning on all the parameters.

$$: L(c, \lambda_0, \lambda_1, P, Q | \Delta p_2, \dots, \Delta p_T) = f(\Delta p_3 | \Delta p_2) \cdots f(\Delta p_T | \Delta \tilde{p}_{T-1})$$

where $\Delta \tilde{p}_{t-1} = \{\Delta p_2, \dots, \Delta p_{t-1}\}$ and

$$\begin{aligned} f(\Delta p_t | \Delta \tilde{p}_{t-1}) &= \sum_{q_t} \sum_{q_{t-1}} f(\Delta p_t | q_t, q_{t-1}, \Delta \tilde{p}_{t-1}) pr(q_t, q_{t-1} | \Delta \tilde{p}_{t-1}) \\ &= \sum_{q_t} \sum_{q_{t-1}} f(\Delta p_t | q_t, q_{t-1}, \Delta \tilde{p}_{t-1}) pr(q_t | q_{t-1}) pr(q_{t-1} | \Delta \tilde{p}_{t-1}) \end{aligned}$$

First the conditional likelihood function $f(\Delta p_t | q_t, q_{t-1}, \Delta \tilde{p}_{t-1})$ is expressed as follows.

$$f(\Delta p_t | q_t, q_{t-1}, \Delta \tilde{p}_{t-1}) = \frac{1}{\sqrt{2\pi\sigma_u^2}} \exp \left\{ -\frac{1}{2\sigma_u^2} \left(\Delta p_t - c \Delta q_t - (\lambda_0 + \lambda_1 \sqrt{V_t}) (q_t - ((P-Q) + (P+Q-1)q_{t-1})) \right)^2 \right\}$$

Second, in order to complete this likelihood function, we need to compute

$$pr(q_t | \Delta \tilde{p}_{t-1}) = \sum_{q_{t-1}} pr(q_t, q_{t-1} | \Delta \tilde{p}_{t-1}) \text{ based on the Hamilton filter. The Hamilton}$$

filter for this model consists of the following:

$$pr(q_t, q_{t-1} | \Delta \tilde{p}_{t-1}) = pr(q_t | q_{t-1}) pr(q_{t-1} | \Delta \tilde{p}_{t-1})$$

We are required to initialize $P(q_1 | \Delta \tilde{p}_0)$ using the steady-state probabilities. In order to get $P(q_t | \Delta \tilde{p}_t)$ for the next iteration, we need to compute the following equations repeatedly for all time t:

$$\begin{aligned} pr(q_t, q_{t-1} | \Delta \tilde{p}_t) &= \frac{f(\Delta p_t, q_t, q_{t-1} | \Delta \tilde{p}_{t-1})}{f(\Delta p_t | \Delta \tilde{p}_{t-1})} \\ &= \frac{f(\Delta p_t | q_t, q_{t-1} | \Delta \tilde{p}_{t-1}) pr(q_t, q_{t-1} | \Delta \tilde{p}_{t-1})}{f(\Delta p_t | \Delta \tilde{p}_{t-1})} \quad \text{and} \end{aligned}$$

$$pr(q_t | \Delta \tilde{p}_t) = \sum_{q_{t-1}} pr(q_t, q_{t-1} | \Delta \tilde{p}_t)$$

where $f(\Delta p_t | q_t, q_{t-1}, \Delta \tilde{p}_{t-1})$ is already given in the above. In sum, an MLE for this model can be developed by summing $f(\Delta p_t | \Delta \tilde{p}_{t-1})$ using the probability terms ($pr(q_t, q_{t-1} | \Delta \tilde{p}_{t-1})$) we computed in the Hamilton filter for each regime over the whole sample.

$$\begin{aligned} L(c, \lambda_0, \lambda_1, P, Q | \Delta \tilde{p}_t) &= \sum_{t=2}^T \ln \left(f(\Delta p_t | \Delta \tilde{p}_{t-1}) \right) \\ &= \sum_{t=2}^T \ln \left(\sum_{q_t} \sum_{q_{t-1}} f(\Delta p_t | q_t, q_{t-1}, \Delta \tilde{p}_{t-1}) pr(q_t, q_{t-1} | \Delta \tilde{p}_{t-1}) \right) \end{aligned}$$

As nested special cases of this model, we can construct the likelihood functions of the Roll and the extended Roll model with autocorrelated q_t as follows.

Case 1) the Roll model with $\lambda_0 = \lambda_1 = 0$ and $P = Q = \frac{1}{2}$

Where $f(\Delta p_t | q_t, q_{t-1}, \Delta \tilde{p}_{t-1}) = \frac{1}{\sqrt{2\pi\sigma_u^2}} \exp\left\{-\frac{1}{2\sigma_u^2}(\Delta p_t - c\Delta q_t)^2\right\}$ and

$$pr(q_t, q_{t-1} | \Delta \tilde{p}_{t-1}) = \frac{1}{2} pr(q_{t-1} | \Delta \tilde{p}_{t-1})$$

Case 2) the extended Roll model with $\lambda_0 = \lambda_1 = 0$

where $f(\Delta p_t | q_t, q_{t-1}, \Delta \tilde{p}_{t-1}) = \frac{1}{\sqrt{2\pi\sigma_u^2}} \exp\left\{-\frac{1}{2\sigma_u^2}(\Delta p_t - c\Delta q_t)^2\right\}$ and

$$pr(q_t, q_{t-1} | \Delta \tilde{p}_{t-1}) = pr(q_t | q_{t-1}) pr(q_{t-1} | \Delta \tilde{p}_{t-1})$$

Appendix D

D. Kim (1994)'s smoothing algorithm.

Given MLE estimates of the model, we can make inferences on the trade direction indicator q_t using all the information in the sample (called smoothing). This gives us the probability of buy-initiated (sell-initiated) trade $\Pr[q_t = 1 | \Delta\tilde{p}_T]$ ($\Pr[q_t = -1 | \Delta\tilde{p}_T]$) for every transaction.

When the models in this paper are estimated by MLE as shown in appendix C, we already utilized Hamilton filter to construct the likelihood function. The Hamilton filter uses the information available up to time t to compute the buy-initiated (sell-initiated) trade at time t , $\Pr[q_t = 1 | \Delta\tilde{p}_t]$ ($\Pr[q_t = -1 | \Delta\tilde{p}_t]$).

Consider the following derivation of the joint probability that $q_t = j$ and $q_{t+1} = k$ based on full information:

$$\begin{aligned} & \Pr[q_t = j, q_{t+1} = k | \Delta\tilde{p}_T] \\ &= \Pr[q_{t+1} = k | \Delta\tilde{p}_T] \times \Pr[q_t = j | q_{t+1} = k, \Delta\tilde{p}_T] \end{aligned}$$

Chapter 4 of Kim and Nelson (1999) explains that $\Pr[q_t = j | q_{t+1} = k, \Delta\tilde{p}_T] = \Pr[q_t = j | q_1 = k, \Delta]$ because if q_{t+1} were somehow known, then $(\Delta p_{t+1}, \Delta p_{t+2}, \dots, \Delta p_T)$ would contain no information about q_t beyond that contained in q_{t+1} and $\Delta\tilde{p}_t$.

$$\begin{aligned} &= \Pr[q_{t+1} = k | \Delta\tilde{p}_T] \times \Pr[q_t = j | q_{t+1} = k, \Delta\tilde{p}_t] \\ &= \frac{\Pr[q_{t+1} = k | \Delta\tilde{p}_T] \times \Pr[q_t = j, q_{t+1} = k | \Delta\tilde{p}_t]}{\Pr[q_{t+1} = k | \Delta\tilde{p}_t]} \\ &= \frac{\Pr[q_{t+1} = k | \Delta\tilde{p}_T] \times \Pr[q_t = j | \Delta\tilde{p}_t] \times \Pr[q_{t+1} = k | q_t = j]}{\Pr[q_{t+1} = k | \Delta\tilde{p}_t]} \end{aligned}$$

and

$$\Pr[q_t = j | \Delta\tilde{p}_T] = \Pr[q_t = j, q_{t+1} = -1 | \Delta\tilde{p}_T] + \Pr[q_t = j, q_{t+1} = 1 | \Delta\tilde{p}_T] \text{ for } j = -1 \text{ and } 1.$$

Given $\Pr[q_T | \Delta\tilde{p}_T]$ at the last iteration of the Hamilton filter, the above can be iterated for $t = T-1, T-2, \dots, 2$ to get the smoothed probabilities, $\Pr[q_t | \Delta\tilde{p}_T], t = T-1, T-2, \dots, 2$

Once we obtain $\Pr[q_t = 1 | \Delta\tilde{p}_T]$ and $\Pr[q_t = -1 | \Delta\tilde{p}_T]$, we can divide the sample into the two regimes using the following rule:

If $\Pr[q_t = 1 | \Delta\tilde{p}_T] > 0.5$, we set $q_t = 1$

If $\Pr[q_t = -1 | \Delta\tilde{p}_T] > 0.5$, we set $q_t = -1$

The above rule is the one we propose to classify the trades. As an illustration purpose, we plot the estimated trade direction indicator series of the extended GH model using the first 1000 observations on May 1.